UNLIMITED

MINISTRY OF DEFENCE

ROYAL

ARMAMENT RESEARCH AND DEVELOPMENT ESTABLISHMENT

REPORT 1/90

Work of Fracture of Composites in Axial Compression – Measurement and Origins

N J Savage

Waltham Abbey
Essex

UNLIMITED

April 1990

CONDITIONS OF RELEASE

0077787 BR-114657

MR PAUL A ROBEY
DTIC
Attn:DTIC-FDAC
Cameron Station-Bldg 5
Alexandria
VA 22304 6145
USA

************************** DRIC U

************************** DRIC Y

Reports quoted are not necessarily available to members of the public or to commercial organisations.

DISTRIBUTION

Internal

1	Director, DD(A), DD(V), SMO, SNO, SAFO - on circulation
2	H/NP
3	H/GS, H/IW, H/EC, H/CA, H/VS, H/VT, H/PM, H/TE - on circulation
4	Dr T J Lewis
5-10	Attn N J Savage, N J Parratt, J Cook, A Howard, M J Hinton, Dr A Groves

External

11	DC(R)
12	DSc(Land)
13	Secretary, Ordnance Board
14	MOD (Whitehall) Library
15-17	DRIC
18	CS(R)2
19-29	Copies for libraries

Overseas

30	USA	DES(W) Director of Munitions
31-32		- DTIC via ONR(L)
33		- Assist Sec of Def (Dept DDR&E)
34-38		- US Army Standardization Group
39	Canada	- DSIS via CDRDS
	Australia	- DSIB via DSTR) (7 microfiche Australia House) copies)

Stock

40-69

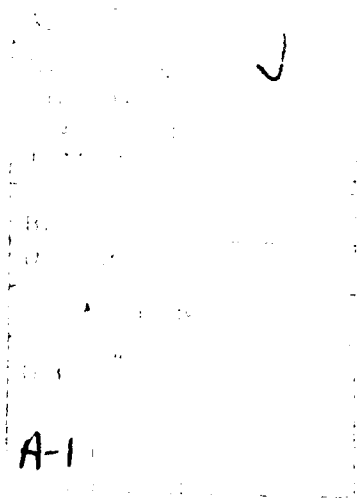

MINISTRY OF DEFENCE

ROYAL ARMAMENT RESEARCH AND DEVELOPMENT ESTABLISHMENT

REPORT 1/90

Work of Fracture of Composites in Axial Compression - Measurement and Origins

N J Savage

Summary

Composite materials are being introduced into weapon systems and launch platforms of many kinds, increasingly as thick sections which accept high compressive stress. A common mode of failure is then by kink band propagation, arising from holes or other stress-raisers. The fibres broken in the process then cause weakness in tension as well. The tolerance of stress-raisers depends upon the energy required to propagate such kink bands.

This report shows how to determine and to adjust this compressive work of fracture, and suggests how much energy different mechanisms may contribute. The work can be as little as 2-3J/cm² when it is concentrated in a narrow band. Multiple kink bands may require up to 400J/cm³ for continuous crushing, an important ballistic feature if it can be sustained.

This report has been accepted as an MSc thesis.

CONTENTS

1 INTRODUCTION

The considerable problems associated with accurately predicting compressive strength in unidirectional continuous fibre reinforced composite materials have been the subject of much attention to date, and the models now available have reached an impressive level of sophistication. The traditional starting point for theories based on elastic instability is Rosen's (Ref 1) theory of in-phase or shear microbuckling which pertains to composites of useful volume fraction. This method equates the strain energies for the unbuckled and buckled conditions using a buckle wavelength which produces the minimum buckling load. This analysis reveals that an upper bound for compressive strength is given by:

$$\sigma_{fcr} = \frac{G_b}{V_f(1-V_f)} + \frac{\pi^2 E_f}{12}\left(\frac{mh}{L}\right)^2 \qquad (1)$$

where σ_{fcr} is the critical fibre stress, G_b is the matrix shear modulus, h is the fibre diameter and L the length, ie L/m is the buckle wavelength. The second term is generally ignored since it is numerically small compared to the first, but its importance may lie in predicting kink band size after microbuckling has occurred. Neglecting this term effectively ignores the contribution from fibre bending, reduces the analysis to a prediction of the shear strength of a set of perfectly straight fibres in a matrix of shear stiffness, G_b, and gives the same result as a virtual work analysis (Ref 2), namely:

$$\sigma_c = G_b/(1-V_f)$$

where σ_c is the composite compressive strength. Because this greatly overestimates values which can be achieved experimentally, subsequent theories of this kind have tended to concentrate on scaling down these values by introducing compensation for such factors as out-of-plane (3D) buckling (Ref 3), imperfections such as fibre bunching and voids (Ref 6), kinked and misaligned fibres (Ref 4), poor adhesion (Refs 4 & 5) and others with varying degrees of success. Rosen's analysis deals in effect with buckling of infinite plates of thickness h, and compensation for the third dimension involves the introduction of an "influence coefficient" (0.63 for the boron/epoxy composite studied in (Ref 3)). Fibre bunching and voids result in a reduction in support against buckling locally and may initiate failure. If the voids are large enough they may cause failure at a greatly reduced stress. Kinked and misaligned fibres may be due to shrinkage stresses on cooling from cure temperature for example, and would lower the microbuckling energy and hence the compressive strength. Poor adhesion or debonding as a result of differences in Poisson's ratio are manifested as a reduced composite shear stiffness. In the limit, for total debonding, the shear stiffness is reduced almost to that of the matrix material full of holes.

Other theories predict strength on the basis of fibre shear failure (Ref 7) in composites with high strength fibres or with brittle matrices, where fibre shear is the lowest energy failure mode, which simplistically states that compressive strength:

$$\sigma_c = 2(V_f T_f + (1-V_f) T_m) \text{ for failure at } 45°$$

where T_f and T_m are fibre and matrix shear strengths respectively.

Work by Weaver and Williams (Ref 8) on unidirectional carbon fibre reinforced plastic (CFRP) indicates that theories based on the Rosen model do not adequately explain variations in compressive strength with superposed hydrostatic pressure or indeed with volume fraction. They suggest a mechanism of kink band formation as a result of microbuckled fibres achieving a critical strain in bending. The kink broadens axially to form a multiply-fractured kink band across the width of the specimen at a characteristic angle of between 20° and 30°. However, similar work by Wronski and Parry (Refs 9 & 10) using superposed hydrostatic pressure suggests that a full width kink band is initiated by a "local surface condition" and that multiple fracturing occurs subsequently. This theory also maintains that in order to obtain agreement with the predictions of Weaver and Williams co-operative buckling of groups of fibres must take place. Some recent experiments by Guynn and Bradley (Ref 11) using quasi-isotropic AS4/PEEK laminates with open holes supports the notion that failure will initiate into an unconstrained region if possible and also explains how the nature of the kink varies from symmetric and asymmetric buckling to shear crippling as shown in Figure 1, depending upon the degree of constraint. The shear crippling (c) type failure produces a sideways displacement of the composite on either side of the failed zone and will occur at or near a free surface where lateral constraint is low. The microbuckling failures involve rotation of the fibres within the damage region, but there is no net lateral displacement. This situation is most likely to occur in more highly constrained areas.

An aspect of compressive failure which has received relatively little attention is that of notch sensitivity. Chaplin (Refs 12 & 13), as early as 1974, suggested that the possibility of notches or other defects, which are present in every composite, acting as stress raisers which might initiate failure through "crack" propagation as happens under tensile loading is potentially as serious as in tension. He suggests a scenario where kinking or "composite shear mode" failure provides a release of stored elastic energy, which drives a compression crease through the material in an unstable manner in common with tension, but with the ameliorating influence of the kinked zone being able to sustain some load. The important point to note here is that before one can happily design structures to operate in compression as well as in tension it is necessary, or at least highly desirable, to know what size of defect is tolerable at the maximum design loads. One way of finding this out in tension is to measure work of fracture, that is how much energy is required to drive a crack through the material. It is then possible, given an appropriate model, to calculate a defect size which, at a particular load, will release just enough energy to drive the crack once initiated. This is the critical defect size. By proposing the

mechanisms of release of stored elastic energy in compression the idea of a critical defect size in compression becomes a valid one. One additional aspect concerned with the proposed ability of these materials to sustain some load after failure is that this only applies to compressive loading. If a structure were also subjected to tensile loading, even though it holds together in compression, it would quickly fall apart in tension. This particularly applies to structures loaded in, for example, flexure. By measuring work of fracture (in fact crack resistance) using end-loaded straight-sided specimens of tapered thickness and an appropriate linear-elastic model based on the double edge-notched pin loaded specimen commonly used for fracture testing in tension, Chaplin attempts to investigate the variation in compressive strength with notch depth for high strength carbon fibre (CFRP) and E-glass fibre reinforced plastic (GRP) composites, and looks at failure initiation and propagation modes and the amounts of energy involved. Figures of between 5 and 10J/cm^2 were obtained experimentally for the propagation energy in CFRP as compared to about 2J/cm^2 by identifying likely energy dissipation mechanisms such as friction, fibre and matrix failure, matrix shear and interface failure, assuming a kink band width of 0.5mm. Clearly other mechanisms are at work which need to be identified.

This very revealing piece of work is limited by the fact that the composite needs to be designed to prevent longitudinal splitting by tailoring the matrix modulus, and so is to a large extent restricted in terms of composition and test conditions. It also proved difficult to interrupt failures in order to allow inspection of the damage zone using sectioning techniques. The use of a very stiff testing machine and a number of spare samples was required.

The main aim of the work described in this report was to design a test piece which could be used with both CFRP and GRP and allow controllable compression failure to be initiated and then interrupted at will under various environmental conditions as well as with different material and lay-up through careful selection of specimen geoemtry. Because of the likely geometric complexity of the resulting specimen this approach does not allow modelling of the stress state imposed, other than possibly using finite element techniques, but it does allow work of fracture to be calculated directly, without the need for a linear-elastic or any other model, by relating the area under the stress-strain curve to the damage surface area provided this is accessible to inspection. After a suitable test piece had been designed and investigated for possible "bugs" it was used to investigate work of fracture in CFRP and GRP, with both unidirectional (ud) and alternative lay-ups.

2 DESIGN OF TEST PIECE

The principal requirements for the test piece were that it should allow propagation of a single compression crease or kink band without creating longitudinal or transverse splitting for both CFRP and GRP in a controllable manner. It should also allow interruption of the test and give an indication of the extent of the damage sustained in order that work of fracture might be calculated. This should be the case for any environmental or material parameters.

The initial idea was that it might be possible to adapt the test piece described by Tattersall and Tappin (Ref 14) for testing brittle materials such as ceramics in tension, for use in compression.

The specimen shown in Figure 2 is "self-stabilising", ie stable crack growth is achieved, because the length of the crack front increases as the crack progresses and so requires increasing amounts of energy in order to propagate. The attraction of this method is that despite the complicated geometry it is possible to extract values for work of fracture because all the elastic energy stored in the beam goes into propagating the crack and the work done is simply the area under the load-displacement curve and the area of damage is the area of the notch, since the test finishes when the sample is completely broken. Work of fracture is then simply the energy divided by the area. Assuming that the hypothesis proposed by Chaplin is correct and that kink band formation releases stored elastic energy which drives the kink further, then by reversing the loading conditions to generate compressive loading at the tip of the cut-away notch and introducing 4-point bending, it was believed that a self-stabilising compressive failure could similarly be attained.

2.1 Materials and Test Equipment

All testing was performed on a J J Lloyd T5002 tensile testing machine using a 4-point bend testing rig with variable large span and a fixed small span of 10mm, under displacement control at a speed of 6mm/min. All the initial specimen design work used Hyfil T300B-R17D5-80 high strength carbon fibre prepreg. The R17D5 resin system is a 120°C curing system based on a DGEBA epoxy resin with a novolac additive. The 80 represents the resin weight per square metre and signifies a low bleed system. This material is of a type typically used for aerospace applications. Subsequent work with GRP utilised Hyfil EGC-195-R17D5-95 E-glass/epoxy prepreg. Both types of laminate were manufactured by compression moulding on to stops in a leaky mould at 200-250 psi, and were cut to size and notched using a lubricated diamond saw.

2.2 Design Details

The first samples tested were those shown in Figure 3a. Large span width was 60mm. The idea was that by using such a wide, flat notch as shown the failure would be quickly stabilised. What happened in fact was that a surface kink was generated at very low load which immediately ran the full length of both sides of the notch owing, it was believed, to the stress-raising effect of the notch surface profile produced by the radiused tip of the 1mm diamond saw blade. Transverse (between plies) and longitudinal splitting also occurred.

The next specimen, shown in Figure 3b, was notched using both a hacksaw blade and a diamond saw blade and was tested using a 60mm span; in neither case did the problem of surface kinking recur. This geometry gave a partially stabilised crack propagation similar to that shown. The initiation load was high, in the region of 2kN. Also shown is the direction of propagation of the compression crease, making an angle of, typically, about 30° to the plane of the notch. This took the failure

band out of the notch leading to destabilisation. Again, both transverse and longitudinal splitting took place. In an attempt to prevent splitting a longer (178mm) specimen of the same cross section was tested using a 120mm span, but instead of splitting being prevented, the additional problem of separation of the fracture face was created, with the fracture face from half of the notch running off at +30° whilst the fracture face of the other half ran off at -30°.

It was felt at this stage that the problem of splitting was a consequence of the ply lay-up direction. In addition the probability of achieving stable crack growth would be increased by reducing the failure initiation load and hence the stored elastic energy available, and this could be achieved by both "sharpening" the notch, ie reducing the included angle, and reducing its cross-sectional area. It was also hoped that the problem of the failure running out of the notch could be prevented by cutting a wider slot using a purpose-made 4mm diamond saw blade.

The specimen geometry which became the standard for the test programme is shown in Figure 3c and in more detail in Figure 4. The large span size used was 100mm. This produced the desired controllable and interruptible compression failures similar to that shown in Figure 5 without splitting and retained the failure within the wider notch.

3 EVALUATION OF TEST PIECE

It was thought necessary that before the specimen described was fully adopted as the standard test piece it should be investigated to ensure that it was performing as expected and that the work of fracture data it would yield were not influenced by factors not yet appreciated. One aspect of the test which differed from that described by Tattersall and Tappin was that because a tensile "hinge" formed on the tensile side of the test piece it would be necessary to halt the test before it reached this stage in order to avoid measuring partly tensile work of fracture. It is therefore necessary to unload the sample to calculate the energy dissipated.

A typical load/deflection curve for CFRP is displayed in Figure 6. The trace was linear between O and A, although the distinct load drop at A did not always occur, and in these cases the linear part of the curve would gradually lean over into stable failure mode. The test could be halted anywhere between B and D and unloaded as shown (CO). The reloading curve followed the line OC. The degree of non-linearity of the unload/reload curve was a function of the amount of damage inflicted, ie almost linear at the level of damage indicated by point B, but highly non-linear at damage level D. One important aspect of the specimen geometry was that if the test piece was turned over so that tensile loading was applied at the crack tip the sample split longitudinally across the full width, opening up the fracture surfaces to inspection and giving a clear indication as to the extent of the damage sustained in compression. This "reverse bending" performance was a major advantage in allowing calculation of damage area because of the distinct separation identified by the splitting. In addition the initial slope of the reverse bending line before splitting occurred is indicated by line OR in

Figure 6, the stiffness being both lower than in forward bending and a function of damage, ie the discrepancy between forward and reverse bending stiffness increased as the level of damage increased.

The fact that both the linearity of the unload/reload curve and the reverse bending stiffness were functions of damage was taken as pointing to a post-failure stiffness as suggested by Chaplin. If this were not the case one might expect the forward and reverse bending stiffnesses to be equal and the unload/reload curve to be linear, albeit both still functions of the degree of damage sustained, as is the case in tension where the crack faces are being pulled apart and load carrying capacity after failure is clearly zero. It is likely that only highly constrained material away from a free edge would offer some load-bearing capacity at reduced stiffness and a model for such a situation is suggested by Guynn and Bradley (Ref 11) and is reproduced in Figure 7. It will be seen later that with this test piece the suggested failure mechanism does not extend further than stage 3, with the fibre fragments making an angle of, typically, 30° to the fibre axis.

Because of the nature of the loading, ie bending, it was feared that such a failure mode might create "crack propping", where failed material is retained in the kink zone and is progressively crushed as the test proceeds so yielding unrealistically high values for work of fracture. It was expected that such a situation would give rise to a damage dependence for the work of fracture - increasing values for increasing damage, and so the initial test programme would test samples at varying levels of damage.

The work of fracture (W) was calculated by halting the displacement at the required level of damage whilst allowing the chart time base to continue. As is evident from Figure 8, a "load drop on stop" occurred. This effect was thought not to be viscoelastic in nature since it was unaffected by loading rate, and so was very likely due to the failure running on a little before stabilising. The amount of load drop on stopping the displacement increased with damage as might be expected if it is indeed due to the crack running on, and considerably more load drop occurred with GRP because of the larger amount of stored energy in the lower modulus fibre. The unloading curve was superimposed on the loading curve using the extrapolated point C as a datum. Hence the work done is the area bounded by the curve OABCO and is calculated manually and converted into the correct units using the appropriate scaling factors. The fracture surface area is estimated by measuring the crack length, h, under a microscope and calculating A using the equation in Figure 9 for the standard specimen geometry.

Clearly it is not possible to calculate exactly the irregular, non-planar fracture surface area any more than it is possible to calculate the surface area of all the pulled-out fibres in a tensile test, so in this respect the assumption is at least as valid as for the tensile test. The fracture surface area is calculated by measuring the crack length, h, from the top of the notch to the tip of the crack after opening the sample up in reverse bending. Errors arising in measuring this length as a result of the non-linear crack front and in reading the microscope vernier scale are of the order of +/- 0.1mm, which are reflected as

errors of about +/- 5% in the work of fracture at 4mm crack length and +/- 10% at 2mm crack length. The errors arising as a result of measurement of area under the load/displacement curve are small in comparison. The graph paper resolution is 1mm², and for a crack length of 2mm in CFRP the enclosed area is typically 600mm².

The initial values of W obtained for CFRP were in the region of 4.5 to 5J/cm² (3 samples) compared to Chaplin's values for crack resistance (R) of between 5 and 10J/cm². This was thought to be an encouraging sign since the discrepancy between known energy dissipation regimes as described earlier and the actual amount of energy dissipated was less than Chaplin had observed.

The test piece had performed satisfactorily during its "road test", and enough confidence had been built up at this stage to allow further testing to be carried out at increasing levels of damage in both CFRP and GRP in order to establish the degree of variability associated with the technique and to ascertain whether crack propping by failed material was a problem.

4 RESULTS

The results of a number of tests carried out at room temperature on unidirectional CFRP and GRP are shown in Table 1.

4.1 Observations

The results for CFRP do not show any obvious correlation between the size of the damage area and the work of fracture. However, the mean value of W for the data set as a whole is 3.93J/cm² with a coefficient of variation of 25.3%, so any trends would be difficult to discern. One possibility is that the data set is bimodal, with most probable values of W at 3.5 and 4.75J/cm² when represented as a histogram as shown in Figure 10. It has already been suggested that the worst case value for experimental error is around 10%. The levels of error likely to arise as a result of variations in material properties are of the same order. With a total error band of about +/- $\sqrt{200}$% the two values suggested are just about significantly different in statistical terms. Clearly more tests would be needed to validate this hypothesis. For the GFRP samples also there is no obvious correlation with damage area, but the actual values obtained for the work of fracture are very much higher than for CFRP, up to three times as high. The two exceptionally high values at minimal damage (samples 6 and 9) can be regarded, for statistical purposes at least, as anomalous because with the GRP specimens a number of separate failures initiate before merging into one damage zone. With this in mind the reduced data set has a mean of 13.78J/cm² and a c of v of 15.3%.

The lack of dependance of W on damage was encouraging in as much as the bend-testing technique employed did not seem to influence the results significantly through crack propping with either CFRP or GRP.

The comparison between the damage zones for the two materials after being unloaded and before being opened up in reverse bending is interesting. Even though the unconstrained surface kinking is not necessarily representative of the failure occurring in the interior of the notch in terms of kink band width and volumetric restraint, clear differences can be identified. In ud CFRP, although the kink does not necessarily proceed linearly down the notch, as can be seen in Figure 15, the width of the band is reasonably constant and fairly small, of the order of 0.25mm. With a scanning electron microscope small bundles of fibres of length varying between 65 and 130 microns can be seen within the damage zone. The SEM pictures for GRP were unsuitable because the lower fibre conductivity caused charging despite the application of a conductive coating. Figure 16, produced using a stereo optical microscope, showed a much larger damage volume. Failure appeared to initiate at a number of sites and propagated over a large width, with delamination spreading some way on either side of the apparent damage zone. Cracks appeared to run along both sides of the notch at the root of the radii left by the slitting saw with delamination and splitting occurring in between. Fibre bundles could not be identified within the damage zone as they were in CFRP. Other workers have observed kink band sizes for these materials which range from 100 to 400 microns for CFRP (Ref 9) and from 250 to 500 microns for GRP (Ref 8). The value for CFRP broadly agrees with the main kink band size of 250 microns seen on the notch surface. The generally smaller lengths of fibre in the debris in CFRP would suggest further fibre fracturing within the kink bands. This aspect will be addressed in detail later.

Examination of the fracture faces themselves using a low power stereoscopic microscope also highlighted differences in failure mode between GRP and CFRP. Near the notch tip and down the notch near a free edge the failure was probably of the shear crippling type seen in Figure 12, which will tend to propagate towards the free edge, and occurs in both materials. However, in the more highly constrained regions in the interior of the notch the picture was different. With CFRP there was evidence of characteristic "terracing", as observed elsewhere (Refs 5 & 10), where whole areas of composite fail perpendicular to the fibre direction on the same level before stepping down parallel to the fibre direction to form the next level. Although the fracture surface was irregular on a macroscopic scale, there was relatively little longitudinal splitting on the microscopic scale. With GRP no such terracing was observed. The surface was extremely irregular with a great deal of splitting in evidence.

It was felt at this stage that because of the extremely high values obtained for work of fracture, especially for GRP, and the excessive scatter in the data, particularly for CFRP, it was necessary to try to formulate some sort of hypothesis based on the data obtained thus far and on any information which might be extracted from higher power microscopic examination before continuing with further testing, both with the present material under normal conditions and with different materials and conditions.

One possible mechanism which it was believed would account for at least some of the extra work done in propagating these compressive failures over and above the theoretical 2J/cm² proposed by Chaplin was the previously mentioned multiple fracturing of kinks. The evidence for multiple fracturing within kink bands is available from a number of sources. Weaver and Williams' (Ref 8) report on CFRP pultrusions under superposed hydrostatic pressure shows micrographs of sections of kink bands where the fibres are broken into very short lengths, typically 20 microns, of "remarkably consistent periodicity". Their explanation for this is that the fibres within the kink band follow simple Eulerian buckling on an elastic foundation which gives rise to a central fracture in bending. The load and the waveform of the buckle would then be transferred along the fibre - "and the process repeated, so that a series of fractures would develop along the length of the fibre". Parry and Wronski (Ref 9) similarly produced some very impressive micrographs of multiply-fractured kink bands under similar conditions of superposed hydrostatic pressure, but disagree with Weaver and Williams, suggesting that this "could well be an artefact of post-failure deformation, rather than relating to kink initiation". Chaplin (Ref 12) also makes some reference to the fibres within the zone breaking into short lengths with associated adhesion failure, but does not include this factor when attempting to explain energy dissipation mechanisms.

It seemed likely that multiple fracturing, occurring as it did under the varying test geometries and conditions described above, was responsible for at least some of the "extra" energy indicated by the figures for work of fracture already obtained. What was not clear from inspection of the fracture faces at low magnification was whether the same type of fracture was being propagated in the test specimen used. Because of the non-planar nature of the fracture surface the most suitable inspection technique was scanning electron microscopy.

In addition to microscopic examination of the fracture surfaces, it was felt that it would be useful to be able to inspect the in-situ compression crease itself after unloading, and to this end the "single-sided notch" sample represented in Figure 11 was produced and tested.

The specimen dimensions were as for the standard test piece, but instead of a v-notch the specimen had a single 4mm slit from the top corner to the opposite bottom corner as shown. Although sectioning techniques would normally be used in this type of situation, this approach was adopted in an attempt to avoid the problems associated with sectioning, namely the amount of effort it consumes and the possible damage to the failed zone, bearing in mind the state of the material contained within it. Even though, being a free edge, it would influence the type of kink which would form, it was hoped that the flat "back" face of the sample would reveal detail about the failure zone which the surfaces of the notch in the standard sample would not.

The SEM micrographs labelled Figures 17-24 are of CFRP and GRP at various levels of damage. For CFRP, characteristic terracing as observed optically can be seen in Figures 17 and 18. The fracture surface is relatively planar away from any free edge with only small amounts of

splitting longitudinally. Figure 19 reveals that co-operative bending failure has occurred at the kink band boundaries, with the fibres failing on the tensile face (Ref 6). It is also apparent from Figures 21 and 22 that some crushing of the matrix occurs both within the kink band (see fibre bundle in Fig 21) and at the boundaries. The SEM photographs of GFRP are again of poor quality. However, it is possible to discern from Figure 23 that the fracture surface is much more irregular than that of CFRP, with extensive splitting and little of the terrace effect seen previously. The fibres still fail through co-operative bending on the tensile face as evidenced by Figure 20, although in this case a wedge of material pops out forming the characteristic cusp seen with glass fibres failed in bending. Figure 24 also reveals some degree of matrix crushing.

The single-sided notch samples in CFRP were quite revealing. The progressive nature of the failure as revealed in Figures 25 and 26 and reproduced diagrammatically in Figure 12 is of interest. It can be seen that the tip of the failure is made up of seemingly one half of a kink band where the fibres have failed almost certainly in bending, and in effect this constitutes a crack. Further back from this the single kink band can be seen with fibre failures along both sides, but with no evidence of multiple fractures at this stage. Behind this is a region of multiple fracture within the kink, with the band broken into 3 or 4 distinct smaller pieces. At the back of the kink at the tip of the cut-away notch the material appears to have fallen out all together. So here is further evidence of multiple fractures in CFRP in a specimen similar to the standard test piece. It cannot be deduced with any certainty in which order the events took place, whether multiple fracturing occurs, leading to the formation of kink bands as proposed by some (Ref 8), or whether it takes place after kinking as a result of the continuing displacement in compression as the test proceeds. The presence of a complete kink directly behind the single crack in Figure 12 lends some support to the latter hypothesis. Neither is it certain what damage and loss of detail result from unloading. What is true is that these arguments are secondary in work of fracture terms since the value obtained is the total package, calculated by measuring the total area within the damage cycle and includes all the energy terms irrespective of their sequence.

The picture is not so clear with GRP. The single-sided specimen does not produce evidence in favour of multiple fracturing. However, the damage zone is extensive, with debonding spreading outside the main crack as with the standard test piece. From the SEM photograph (not shown) it is just possible to identify fibre bundle fragments of the order of 340 microns, which is in the middle of the range of surface kink sizes for GRP seen elsewhere.

4.2 Initial Hypothesis

It has been established both from reference to other work and from the work described above that multiple fracturing does occur within kink bands under normal circumstances rather than in exceptional ones. What is still not clear is why. Why does the crack formed by one half of the kink band fracturing not run on under the influence of its own stress

concentration as is the case in tension for brittle materials? The answer might well be that crack deflection occurs which partially blunts the stress concentration as tends to happen in tension in composites with an optimum level of adhesion. The crack then has to restart before continuing. Crack deflection is responsible for increasing the work of fracture in tension through blunting of the crack tip principally at the fibre/matrix interface, and the same may be true for composites in compression, with similar results. If this were so then the explanation of the behaviour of CFRP would be that as a result of crack deflection and crack tip blunting the crack becomes more demanding in energy terms and requires more compressive displacement in order to continue, resulting in further splitting of the kink band into a relatively small number of smaller pieces. This number is variable and results in a bimodal, or worse, distribution of values for work of fracture with a high degree of scatter. GRP on the other hand undergoes much more extensive crack deflection resulting in the rather complex fracture mode which has been observed, but producing a lower level of scatter in the data. The reasons for the differences between CFRP and GRP are the inferior adhesion between glass and epoxy compared to carbon fibre and the larger amounts of stored elastic energy in the lower modulus glass fibre composite, which together give rise to extensive debonding over a significantly larger area. However, it may be that the total energy per unit volume damaged for the two materials is broadly similar.

In order to validate the above hypothesis it was decided to experiment with a number of different lay-ups which should either increase or decrease the compressive work of fracture. In decreasing the work of fracture the aim is to reduce the amount of splitting to the point where a single kink band or even half kink is propagated, so putting a number on the minimum possible value for the particular lay-up. By using the lower lay-up shown in Figure 13 it was expected that the presence of the 90° plies would serve to confine crack deflection and any subsequent longitudinal or transverse splitting to within the two 0° plies between each successive set of 90° plies. The most significant reduction in work of fracture should clearly occur with GRP since it is believed that the very high values are due to extensive crack deflection. If a single kink band were to be generated the value should fall to the same level as for CFRP or lower. Because much less crack deflection occurs in CFRP the effect should be less pronounced, but some improvement on the scatter of the data for the unidirectional material is expected. What effect the inclusion of 90° plies in the lay-up will have on the intrinsic work of fracture is difficult to estimate with any certainty. By analogy with crack propagation in tension, the crack opening mode (mode 1) consumes the lowest amount of energy and any change in lay-up which changed failure mode would tend to increase the crack propagation energy. However, the composite shear failure which results in kink band formation is more akin to forward shear (mode 2) or possibly even mode 3 type failure. Assuming this to be true, it is likely, therefore, that inclusion of 90° material will not significantly affect the work of fracture in its own right.

The lay-up designed to increase work of fracture would do so by promoting additional crack deflection and splitting at the interfaces between the 0° and 90° plies in GRP and the 0° and 45° plies in CFRP. The lay-ups for the two materials differ because it was thought that the shear coupling afforded by the +/- 45° layers might reduce the amount of splitting which occurred and the CFRP would be the more sensitive barometer for any such effect, since less splitting occurs in the unidirectional material. The greatest increase in W would be expected in CFRP for the same reason.

4.3 Results for Bi-Directional Lay-Ups

The results of the tests on the lay-ups designed to reduce work of fracture in CFRP and GRP are shown in Table 2.

The results for the tests on the samples intended to increase work of fracture are:

CFRP (mean of 2) = 8.45J/cm²

GRP (mean of 3) = 14.77J/cm²

4.4 Discussion

Considering the lay-up designed to reduce work of fracture, from the limited number of tests performed it would appear that the mean value for CFRP is essentially the same as for the unidirectional material, although there is some evidence that the scatter is lower, with a c of v of 13.3% compared to 25.3% for the whole ud data set. It could be seen clearly using a lower power stereomicroscope that splitting was taking place at the interfaces between the two ply directions, and it may be that this approximately cancels out any reduction in crack deflection. The fracture surface was somewhat more planar than that of ud material as can be seen in Figures 27 and 28.

The section of material seen in Figures 29-31 is taken from the fracture surface at the interface between the two fibre directions and away from a free edge. It is clear from these photos that more than just a single kink has propagated. The "V" formed by the kinked fibres was inclined towards the tip of the notch section, suggesting that the material has rotated against the direction of failure propagation and into a failed region as might be expected, rather than into an undamaged region. The length of a single fibre which forms one half of the "V" is in the range 30 to 65 microns. The fragments of the kink were extremely fragile, indicating extensive and intense matrix damage. Evidence of this can also be seen in Figure 32, which highlights a similar situation in another sample that has fibre fragments in the range 25-45 microns. A single-sided sample also revealed evidence of what up to know has been taken to be a multiply fractured kink band.

The results for GRP show a clear reduction in the work of fracture, with the mean value less than half that for ud GRP. Inspection of the unloaded sample revealed that after a "messy" start at the notch tip, where a number of cracks initiated, the main failure propagated apparently as a single half-kink as indicated in Figure 33. The damage

volume was substantially less than for ud material, with no evidence of debris within the kink band, but with some debonding outside the crack. However, similar cracks also propagated for some way along both of the radii produced by the slitting saw. This occurred with all the samples tested. It was felt at this stage that in order to reduce the work of fracture further by eliminating these unwanted failures, a specimen redesign was necessary and would involve widening the notch even more and increasing the saw tip radii to reduce the stress concentrations it produced. This would not be attempted in the present programme of work. Even though the values obtained were higher than expected because of the geometric problems encountered, it is clear that the lay-up adopted did significantly reduce the amount of crack deflection and splitting which occurred, as witnessed both by the volume of the damage zone when examined externally (Fig 33) and by the more planar fracture surfaces seen in Figures 34 and 35. It may be that, had the single crack indicated propagated alone, the work of fracture obtained would have been very low indeed, probably lower than that for CFRP.

The alternative lay-up designed to increase work of fracture also behaved largely as expected, giving a twofold increase in the value for CFRP, although the GRP value was unaffected. In both cases extensive splitting occurred at the 0/90 or 0/45 interfaces. Examples are shown in Figure 36 for CFRP and Figure 37 for GRP.

4.5 Revised Hypothesis

The series of tests described above using different lay-ups tailored to increase or reduce the work of fracture increased confidence in the belief that crack deflection followed by splitting was responsible for dissipation of at least some of the energy so far unaccounted for. What is still not resolved is the question of multiple fracturing of the kink bands. If this process occurred after the formation of the main kink, ie after the fibres within it had rotated at an angle to the loading direction, it is unlikely that subsequent displacement, either as a result of release of stored energy or as a result of further controlled compression of the kink band surfaces, would give rise to such regular fracturing as has been observed both here (Fig 12) and elsewhere (Refs 9, 10 & 12) for CFRP composites. On the other hand, the suggestion (Ref 8) that very small microbuckles, of the order of 20 microns, grow into kinks of the size generally observed is not supported by the fact that complete, unfragmented bands have been seen in this work (Fig 12) and elsewhere (Ref 9). In addition, fibre fragments as small as 20 microns and of the regularity suggested have not been seen in any of the SEM micrographs.

These facts have prompted the idea that the fibre fragments of about 40 microns in length seen in CFRP are in fact the remains of individual kink bands. When crack deflection occurs the additional energy requirement and so the extra displacement cause further kink bands to form one on top of the other. The single, large kink seen in the single-sided test (Fig 12) is probably the result of the top kink running on a little after stopping the displacement. With unidirectional GRP the extensive splitting tends to prevent the formation of such neat failure bands, and in the bidirectional GRP only a single half-kink seems to propagate in any case.

What sort of kink band widths are predicted for these materials by the various theories looked at so far? It should be possible to use these theories to predict whether kink band size is of the order of 40 microns as suggested, or whether it is in the range 100-400 microns for CFRP and 250-500 microns for GRP as reported elsewhere (Refs 9 & 10).

It has been suggested earlier that the often neglected second term in Rosen's formula for in-phase microbuckling (equation 1) is useful in predicting buckling wavelength. It is in fact a specific solution of the Eulerian buckling equation given in Annex A. It has already been stated that the left hand term in the equation is dominant in determining composite failure. The right hand term, however, will dictate the buckling wavelength once the fibres have achieved critical stress, ie when the composite shear term can be put at zero, and this can be expressed in the equation:

$$L/m \text{ or } l = \pi h\sqrt{(E_f/12\sigma_f)} \qquad (2)$$

For CFRP, from the data sheet for the system used, h=7 microns, E_f=230 GPa. The value for fibre strength is generally determined by measuring the compressive strength of the composite itself and relating it to fibre strength knowing the volume fraction. In this case, because of the complicated specimen geometry, this was not possible. Assuming a low value of 1000 MPa for the composite compressive strength and volume fraction of fibre of 60%, the buckle wavelength using the above equation is 75 microns. The kink band widths, which are half the buckle wavelength, suggested by the SEM photographs of the $(0_2/90)_{1s}$ lay-up (Figs 29-32) form a range of values between 30 and 45 microns. Figures 38 and 39 which show the fracture surface of ud CFRP, also reveal kink bands of lengths between 38 and 58 microns. The two values from theory and observation broadly agree, lending weight to the suggestion that the intrinsic kink band width for the material is about 40 microns. Equation 2 also implies that the band width for GRP will be smaller. Typical values for E-glass are (Ref 6), h=10 microns, E_f=76 GPa. When a value of 1000 MPa is used for compressive strength (Refs 9,13), the buckle wavelength is about 60 microns. No photographic evidence was found to corroborate this.

Turning again to energy considerations for composite shear failure and applying these new, smaller values for kink band width, it has been suggested that the principal sources of energy dissipation are matrix deformation (W_m) and fibre/matrix debonding (Ref 12) (W_d). The energy sum then takes the form:

$$\text{Work of Fracture, } W = W_m + W_d + W_e$$

where W_e is the stored elastic energy in the kink band before fibre failure. Assuming a worst-case scenario for GRP, ie all the stored energy goes into driving the crack, and assuming a somewhat larger than predicted kink band width of 50 microns:

$$W_e/\text{unit volume} = E_e^2/2$$

where E is the fibre modulus and e the strain. The maximum fibre strain will be no more than 6% in tension at the kink band boundaries with a mean fibre stress within the kink band of perhaps 4%, giving a value for:

$$W_e = 76\times10^9 \times 0.04^2 \times 50\times10^{-6}/2 = 0.3 J/cm^2$$

The matrix deformation work:

$$W_m = t\gamma T_y(1-V_f) \qquad \text{(Ref 12)}$$

where t is the band width, γ is the shear strain, T_y the matrix flow stress during plastic deformation. Microscopic examination of fibre bundle fragments indicates a shear strain of about 30°. Assuming a worst case of 45°, and using a flow stress of 50 MPa (Ref 12):

$$W_m = 50\times10^{-6} \times 1 \times 50\times10^{-6} \times 04 = 0.1 J/cm^2$$

The work of interface debonding:

$$W_d = 2tV_fW_{mf}/r \qquad \text{(Ref 12)}$$

where W_{mf} is the fibre/matrix debonding energy and r the fibre radius. Using the value for mode 2 interlaminar fracture (Ref 15) for W_{mf} and assuming total debonding of all fibres within the kink:

$$W_d = 2 \times 50\times10^{-6} \times 0.6 \times 400/5\times10^{-6} = 0.48 J/cm^2$$

The total energy budget for all the terms so far addressed is less than $1 J/cm^2$. Repeating the sum for CFRP, bearing in mind the lower strain to break of the higher modulus fibres and the somewhat larger value for W_{mf} (Refs 16 & 17), and assuming a slightly larger kink band size of 60 microns, a comparable low value for the total energy dissipation results:

$$W_e = 230\times10^{-9} \times 0.015^2 \times 60\times10^{-6}/2 = 0.16 J/cm^2$$

$$W_m = 60\times10^{-6} \times 1 \times 50\times10^{-6} \times 0.4 = 0.12 J/cm^2$$

$$W_e = 2 \times 60\times10^{-6} \times 0.6 \times 500 \,/\, 3.5 \times 10^{-6} = 1.03 J/cm^2$$

$$W_{cfrp} = 1.31 J/cm^2$$

Taking these worst case figures, it is conceivable that the values for work of fracture measured for CFRP could be the result of the formation of multiple kink bands, 3 or 4 of them, piled up to form the type of failure band seen in the single-sided samples (Fig 12). However, from the photographic evidence (Fig 21) it is clear that total debonding is not taking place within the kink band. Since this is the largest energy term it is likely that some other dissipative mechanisms is operating. Figures 21 and 22 show evidence of damage to the matrix, both within the kink and at the boundary, which is not the result of either debonding or plastic flow. It is suggested that matrix crushing is also occurring as indicated in Figure 14.

Clearly the fibre spacing shown is exaggerated. However, this sort of matrix pulverisation resulting from continuing compressive loading on a material which is able to undergo only limited plastic flow would give rise to the condition seen in Figures 21, 22 and 40.

For GRP the neat multiple kinks described have not been observed. What is apparent, however, is that some degree of debonding does occur outside the kink bands (Figs 16, 33, 37), particularly in the unidirectional material. Using a larger value for the band width in the debonding work equation to include this larger damage volume will significantly affect the total energy sum, but in order to account for the measured work of fracture value for ud GRP total debonding would have to take place over a damage width of around 1mm. It is likely that matrix crushing also occurs in GRP and evidence for this can be seen in Figure 24.

The values for mode 2 or 3 crack propagation for the untoughened epoxy resin system used are typically a few hundred J/m^2. The constraint offered by the fibres may increase this to some extent. However, total energy dissipation as a result of matrix crushing could be substantial due to the total area of cracking involved.

5 CONCLUSIONS

The initial aim of this programme of work was to design a simple test specimen for measuring work of fracture in compression for various materials under different environmental conditions. The test geometry settled upon as the standard can certainly be considered a success when used for testing the CFRP material under normal conditions. Fabrication is simple and testing does not require the use of specialised machinery or grips and attachments. The results obtained for ud material are reasonable in the sense that the amounts of energy dissipated can be accounted for as described in Section 4.5. The scatter of results can be reduced by using the lay-up designed to reduce crack deflection.

With GRP the geometry chosen was less successful. The formation and propagation of failure were heavily influenced by the radii left by the slitting saw used to cut the notch. This problem would be alleviated by increasing the notch width and increasing the saw edge radii. Even so, clear differences did emerge between CFRP and GRP in terms of the amount of crack deflection taking place and in the volume of the damage area, and this was reflected in the very high values recorded for ud GRP. The lay-up designed to reduce splitting in GRP had a significant effect on the values for work of fracture despite the interference from the edges of the notch.

The hypothesis proposed states that crack deflection occurs as failure progresses, blunting the crack tip and requiring more displacement to occur in order to drive the crack further. In CFRP this has the effect of creating multiple kinks of the order of 40 microns in length which pile up on top of one another. In ud GRP, because of the extensive splitting which takes place, this effect is not observed, although kink band formation does occur in a more random fashion as witnessed by the bending failures seen on the fracture surfaces. When the lay-up is tailored to reduce crack deflection the splitting is drastically reduced to the point where a single half-kink or very narrow kink is seen to propagate.

It was not possible in the time available to carry out testing under different environmental conditions and using different materials. However, conducting a single test at reduced and elevated temperatures seemed to indicate that no significant effect is seen at 0°C, either for GRP or CFRP, whereas testing at 100°C significantly increases the work of fracture for GRP only.

One interesting point of speculation which arises from the fibre buckling equation 2 is that by using stronger fibres in the composite the buckling wavelength and hence the work of fracture decrease, all other things being equal. The implication is that in order to increase compressive strength without increasing notch sensitivity it is necessary to use larger diameter fibres. This is one aspect of the work that could usefully be investigated.

6 REFERENCES

1 Rosen B W — Mechanics of Composite Strengthening, Presented at a Seminar of the American Society of Metals, Oct 1964.

2 Parratt N J — Fibre Reinforced Materials Technical, Van Nostrand Reinhold, 1972, p46.

3 Lager J R, June R R — Compressive Strength of Boron Epoxy, Journal of Composite Materials, 3, p48, 1969.

4 Piggot M R et al — The Compression Strength of Composites with Kinked, Misaligned and Poorly Adhering Fibre, Journal of Materials Science, 16, p2831-2845, 1981.

5 Steif P S — A Simple Model for the Compressive Failure of Weekly Bonded, Fibre-Reinforced Composites, J of Comp Mats, 22, p818, 1988.

6 Hull D — An Introduction to Composite Materials, CUP 1981, Cambridge Solid State Science Series.

7 Ewins P D, Ham A C — The Nature of Compressive Failure in Unidirectional Carbon Fibre Reinforced Plastics, RAE Technical Report 73057, 1973.

8 Weaver C W, Williams J G — Deformation of a Carbon-Epoxy Composite Under Hydrostatic Pressure, Journal of Materials Science, 10, p1323, 1975.

9 Wronski A S, Parry T V — Compressive Failure and Kinking in Uniaxially Aligned Glass-Resin Composite Under Superposed Hydrostatic Pressure, J of Mat Sc, 17, p3667, 1982.

10	Parry T V Wronski A S	Kinking and Compressive Failure in Uniaxially Aligned Carbon Fibre Composite Tested Under Superposed Hydrostatic Pressure, ibid, p893.
11	Guynn E Gail Bradley W L	A Detailed Investigation of the Micromechanisms of Compressive Failure in Open Hole Composite Laminates, J of Comp Mats, 23, p479, 1989.
12	Chaplin C R	A Study of Compressive Fracture in Unidirectional Fibre Composites, University of Reading, MOD(PE) Contract No AT/2035/012/MAT, 1975.
13	Chaplin C R	Compressive Fracture in Unidirectional Glass Reinforced Plastics, J of Mat Sc, 12, p347, 1977.
14	Tattersall H G Tappin G	The Work of Fracture and its Measurement in metals, Ceramics and Other Materials, J of Mat Sc, 1, p296, 1966.
15	Verbruggen M L C E	Paper Presented at ICCM 6, Imperial College, London, 1987, Volume 5, p5.461
16	Sela N Ishai O	Interlaminar Fracture Toughness and Toughening of Laminated Composite Materials: A Review, Composites, 20, 5, Sep 1989.
17	Russell A J Street K N	Moisture and Temperature Effects on Mixed Mode Delamination Fracture of UD Graphite-Epoxy, ASTM STP 876, p349, 1985.

TABLE 1

CFRP Work of Fracture

Sample No	Damage Area (mm^2)	Work of Fracture (J/cm^2)
20	1.04	3.10
17	2.13	3.45
15	2.34	4.76
21	3.73	4.77
18	3.88	2.40
22	4.17	3.57
14	4.47	3.50
19	4.47	2.92
16	6.51	4.84
23	8.51	4.29
24	10.77	5.65

GRP Work of Fracture

Sample No	Damage Area (mm^2)	Work of Fracture (J/cm^2)
6	0.64	31.79
9	1.04	20.83
5	3.73	13.28
4	4.47	13.90
8	4.47	14.14
11	5.44	9.30
10	5.62	14.93
13	6.51	16.84
2	6.70	12.18
12	7.28	14.12
3	8.30	16.14
1	12.25	13.00

TABLE 2

CFRP Work of Fracture $(0_2/90)_{16}$

Sample No	Damage Area (mm^2)	Work of Fracture (J/cm^2)
1	7.68	4.42
2	8.09	4.40
4	7.68	3.84
5	9.83	5.36
6	7.15	4.02
S D = 0.59	Mean = 4.41J/cm²	c of v = 13 3%

GRP Work of Fracture $(0_2/90)_{16}$

Sample No	Damage Area (mm^2)	Work of Fracture (J/cm^2)
3	7.08	6.98
4	6.51	7.47
5	6.89	5.48
S D = 1.04	Mean = 6.64J/cm²	c of v = 15.6%

FIGS. 1 & 2

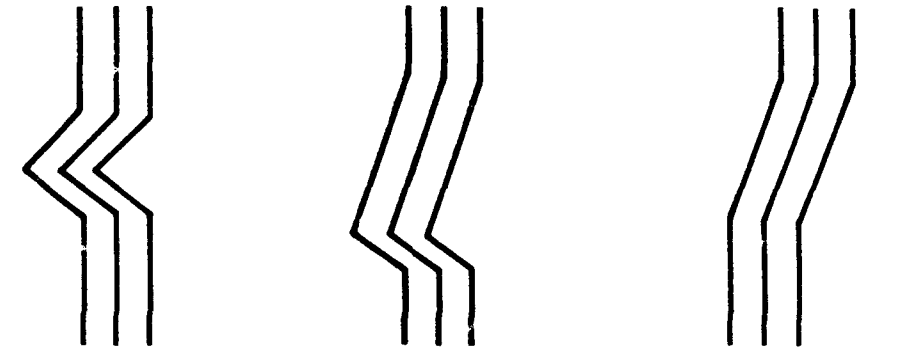

FIG. 1

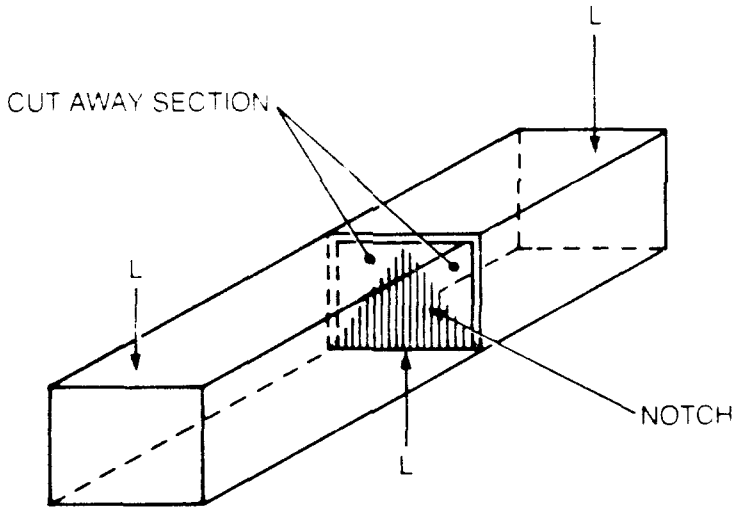

FIG. 2 TATTERSALL AND TAPPIN TEST PIECE

FIGS. 3a.b & c

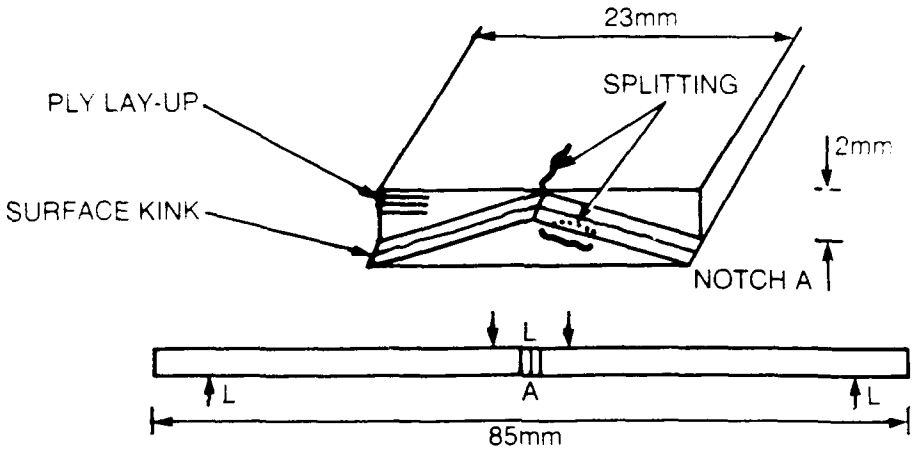

FIG. 3a

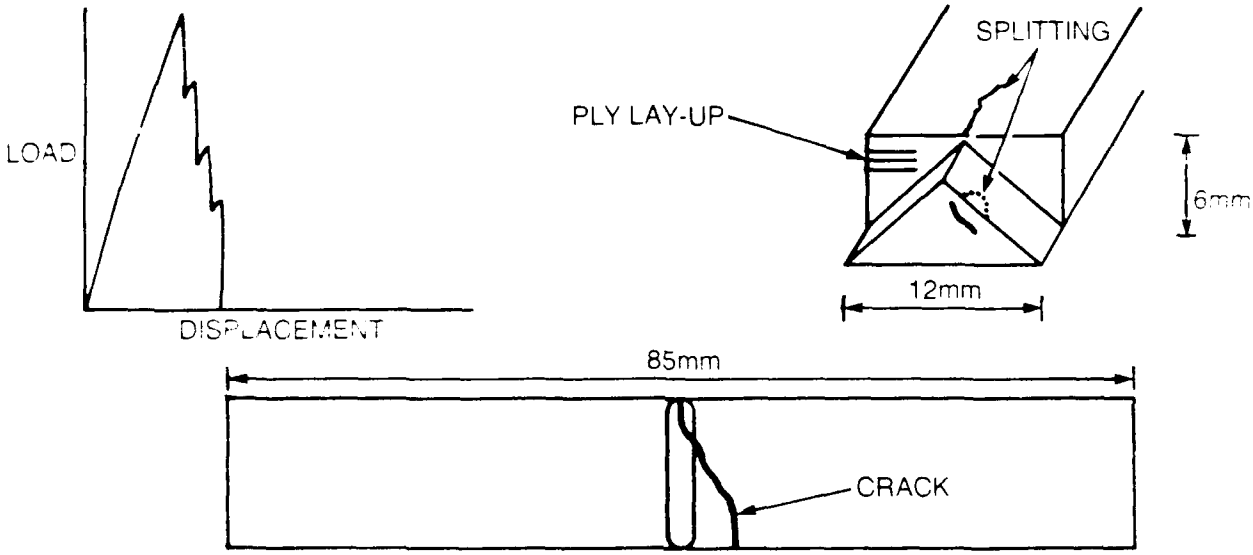

FIG. 3b

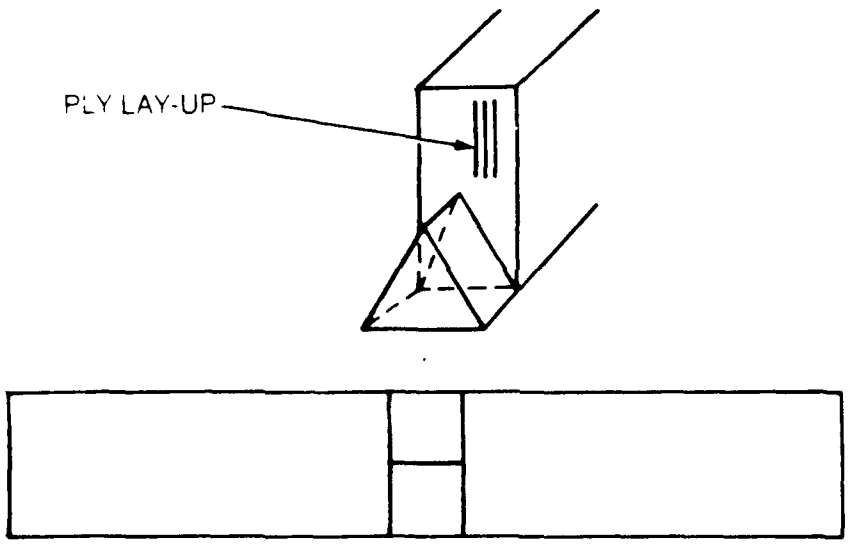

FIG. 3c

FIGS. 4 & 5

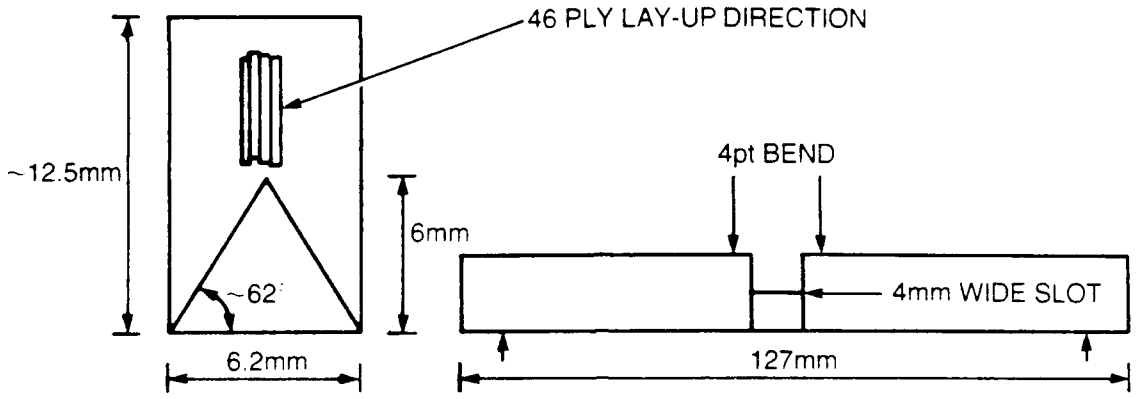

FIG. 4 TEST SPECIMEN

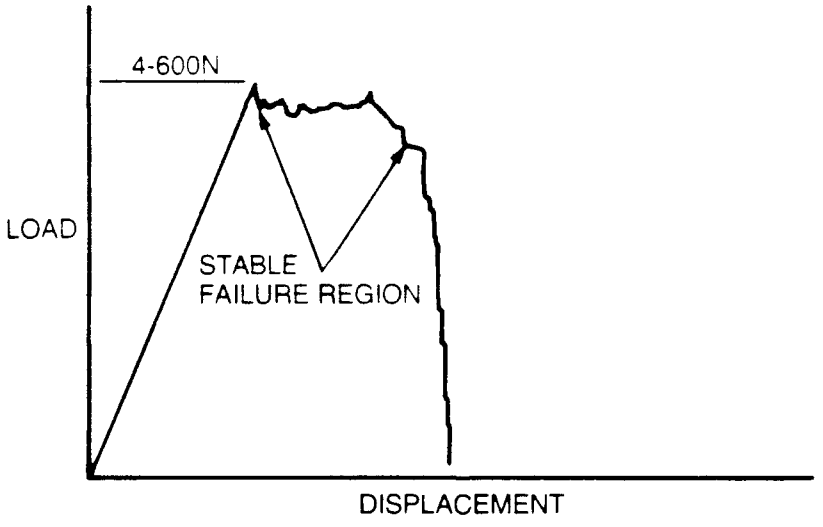

FIG. 5

FIGS. 6 & 7

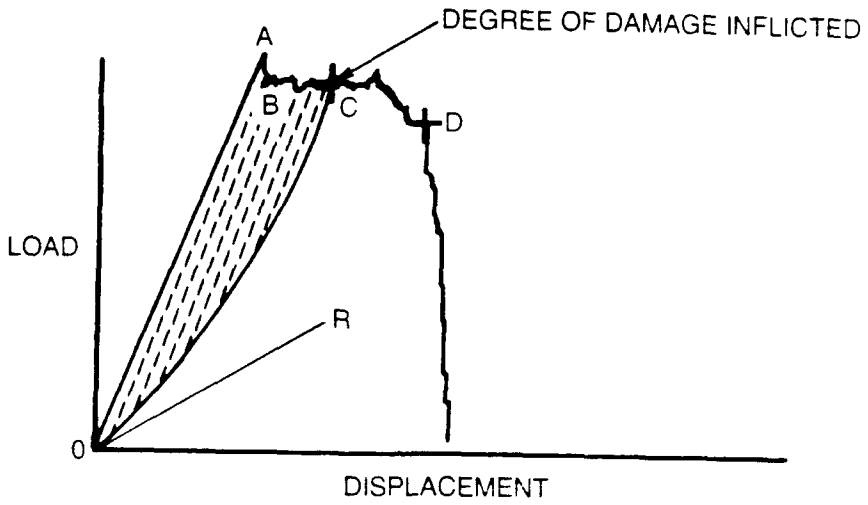

FIG. 6

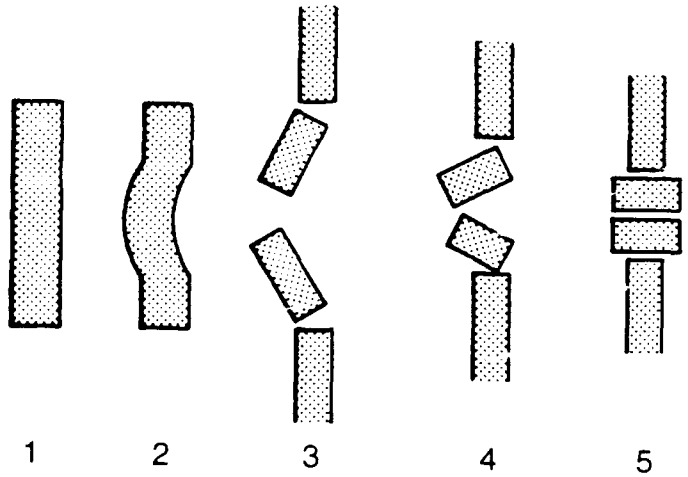

FIG. 7

FIGS. 8 & 9

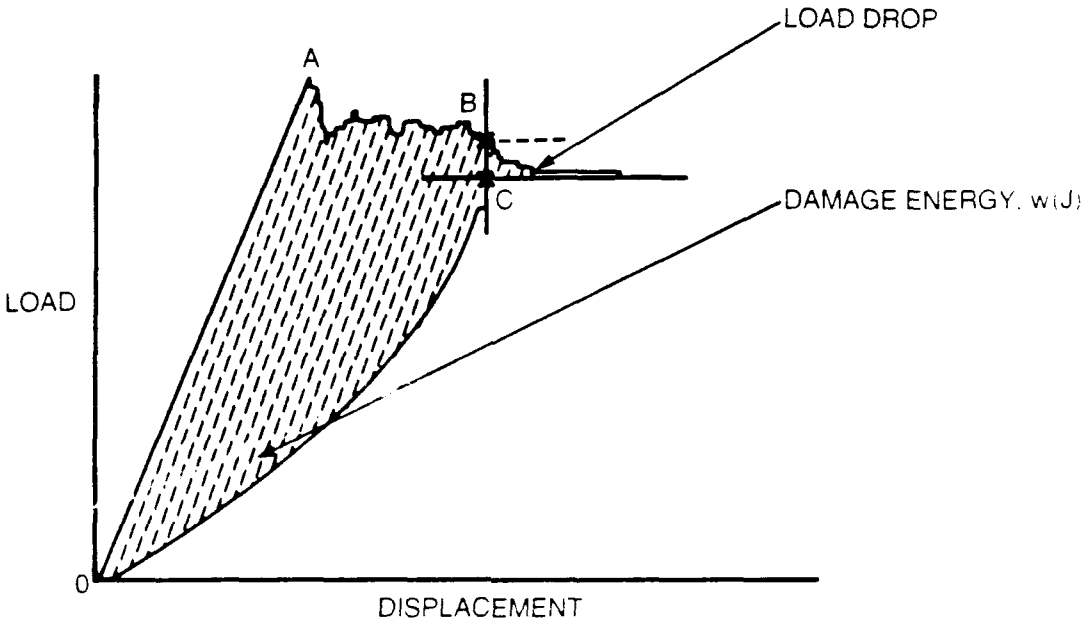

FIG. 8

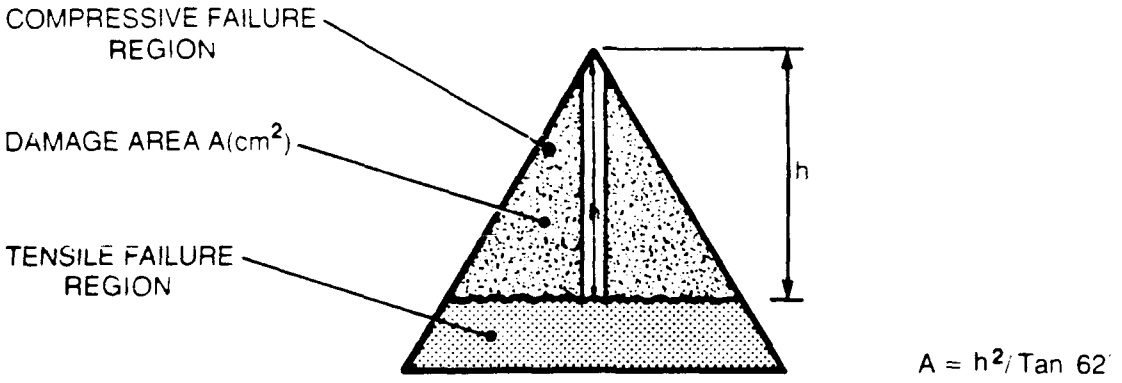

WORK OF FRACTURE, W = w /A (J/cm²)

FIG. 9

FIGS. 10 & 11

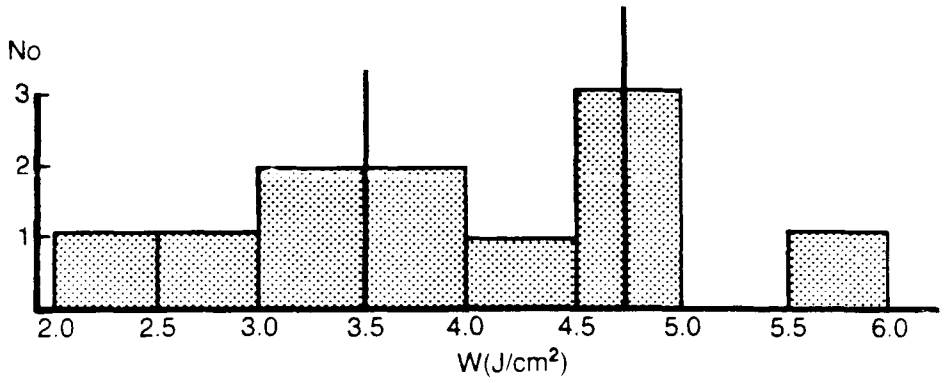

FIG. 10

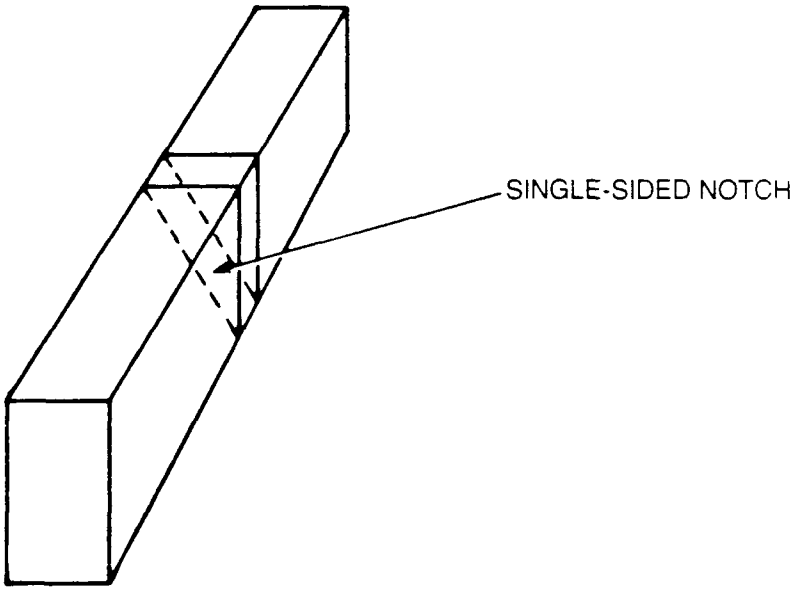

FIG. 11 SINGLE-SIDED SPECIMEN

FIGS. 12 & 13

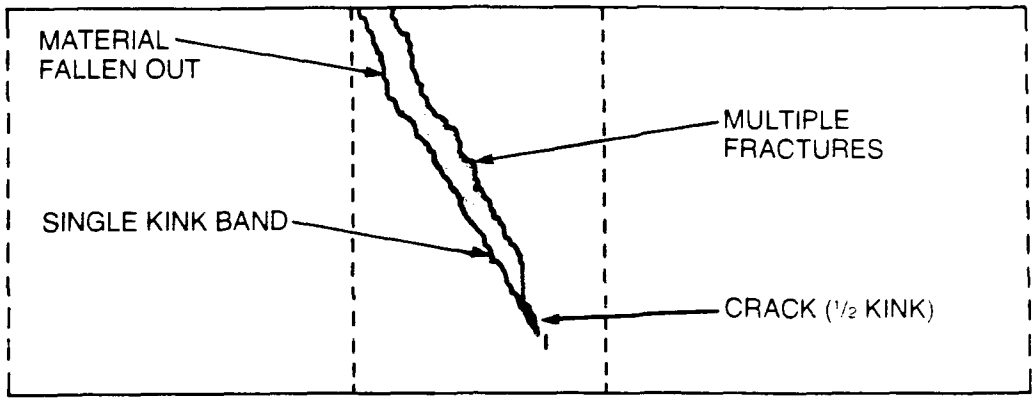

FIG. 12 BACK EDGE OF SINGLE-SIDED SPECIMEN

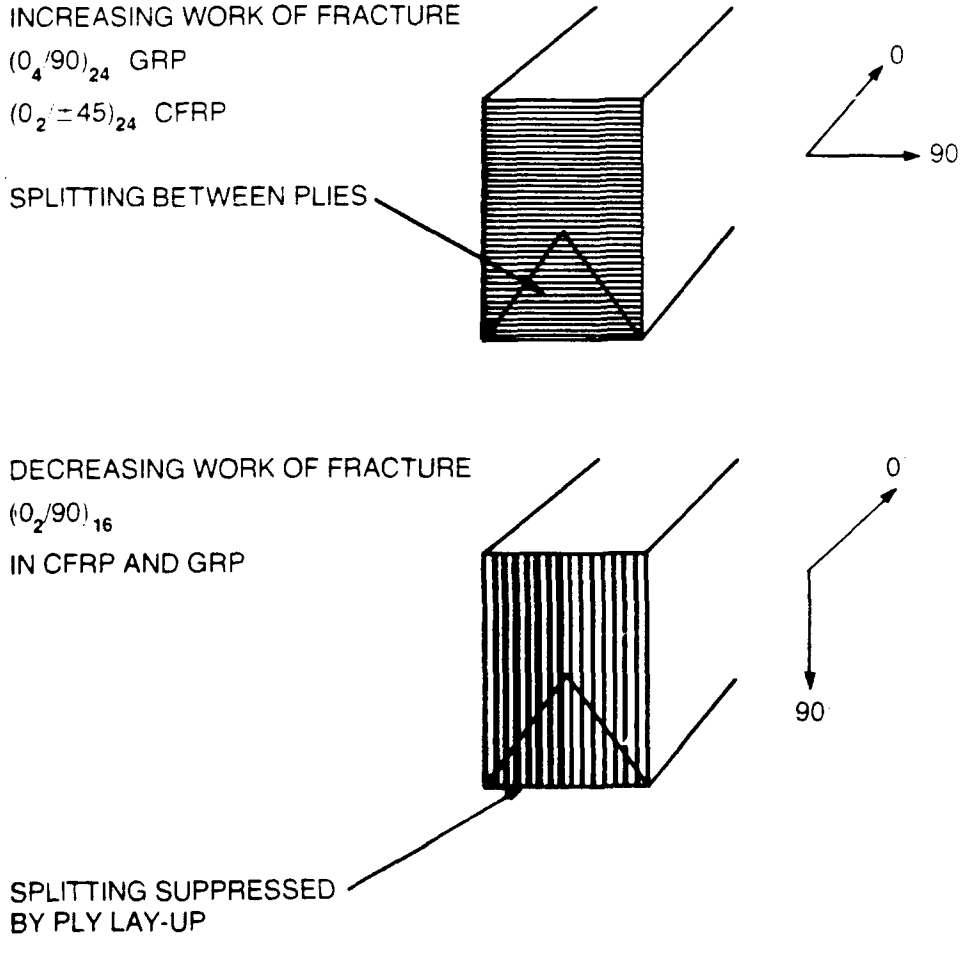

FIG. 13

FIG. 14

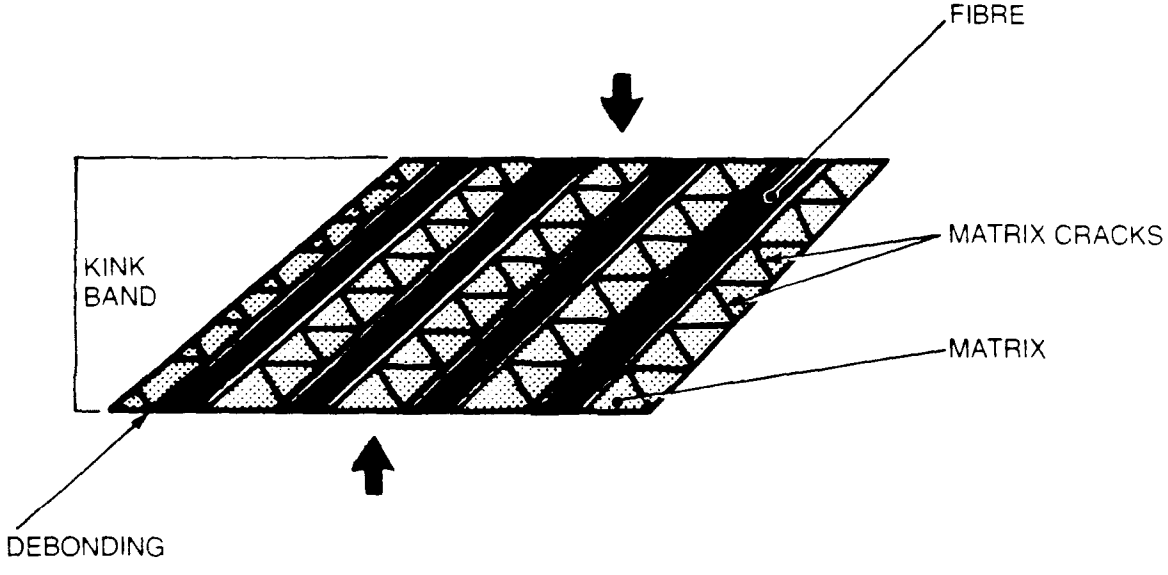

FIG. 14 POSSIBLE MECHANISM FOR MATRIX CRUSHING

FIG 15

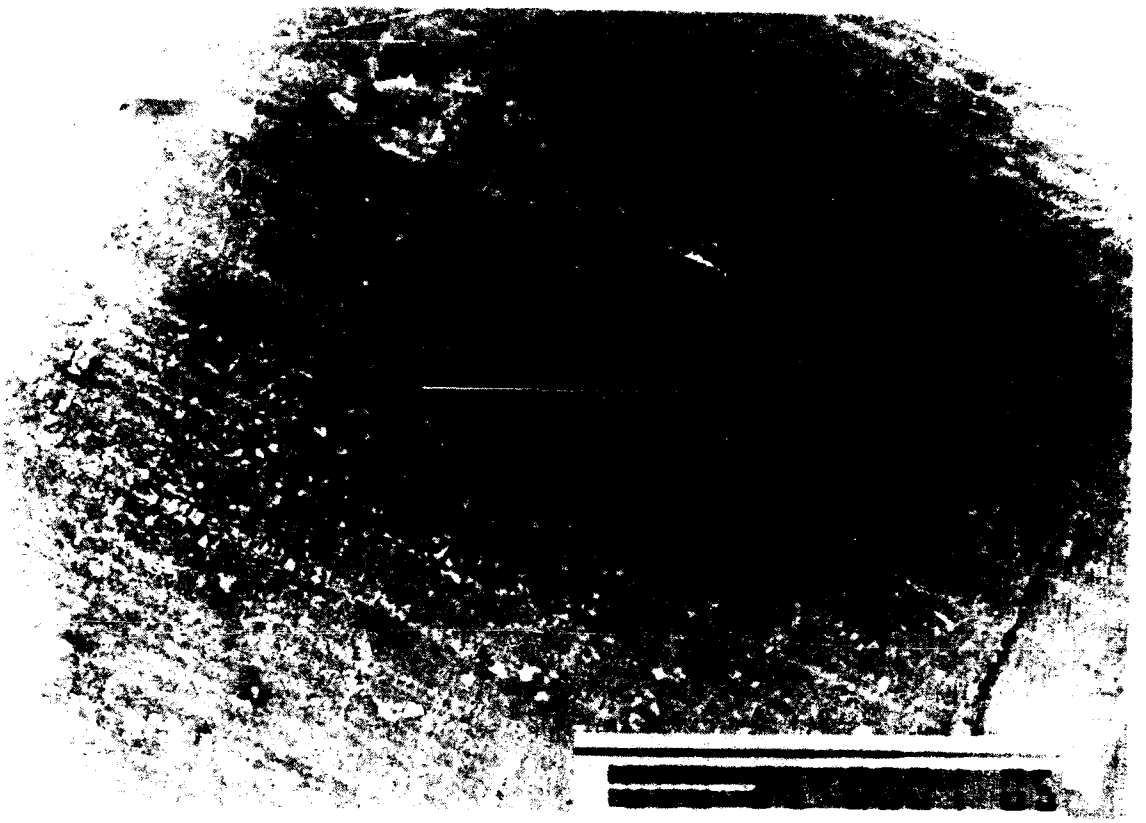

FIG 15 SURFACE KINK IN UNIDIRECTIONAL CFRP STANDARD SPECIMEN

FIG. 16

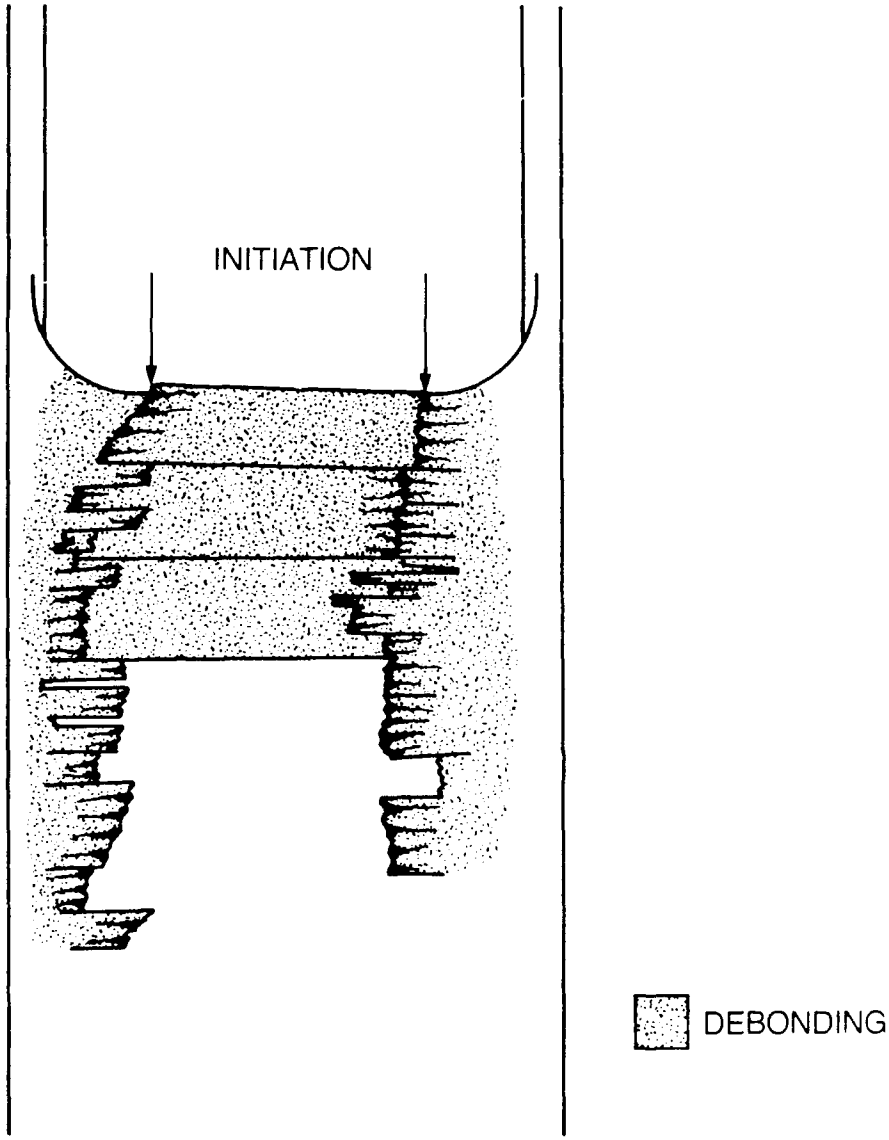

FIG. 16 SURFACE OF UD GRP STANDARD SPECIMEN

FIG. 1[illegible] x 50)

FIG. 18 (x 200)

FIGS. 17 & 18 TERRACING IN UNIDIRECTIONAL CFRP

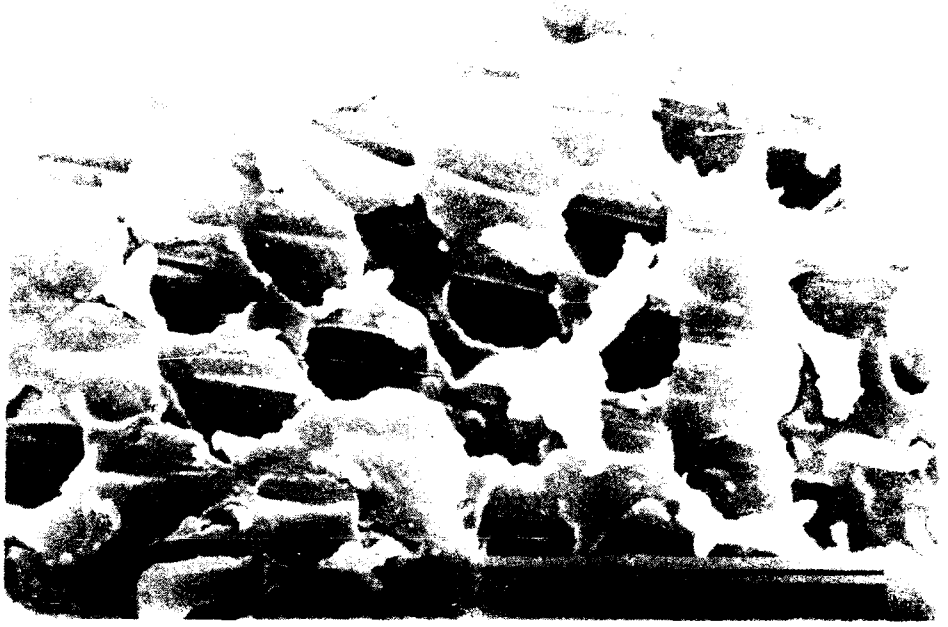

FIG. 19 (x 2000)

FIG. 20 (x1000)

FIGS. 19 & 20 BENDING FAILURES IN CFRP AND GRP

FIG. 21 (x750)

FIG. 22 (x 2000)

FIGS. 21 & 22 MATRIX CRUSHING IN CFRP

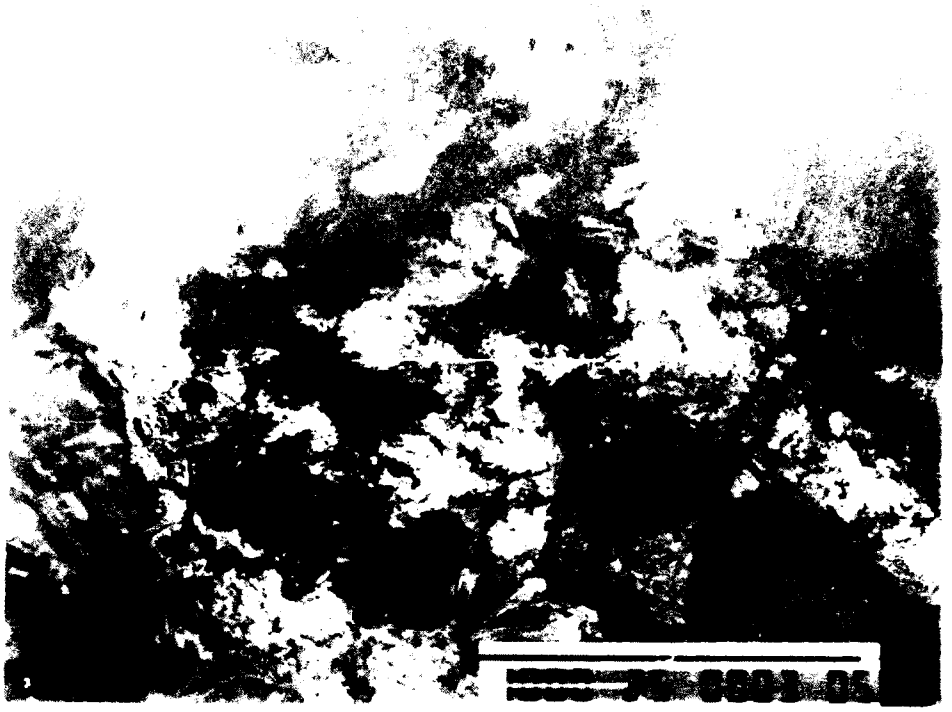

FIG 23 (x 50)

FIG 24 (x 350)

FIGS 23 & 24 SPLITTING AND MATRIX DAMAGE IN GRP

FIG. 26 DETAIL TO TIP OF CRACK IN SINGLE-SIDED
[illegible] SPECIMEN

(X 35)

FIG. 27 FRACTURE SURFACE OF $(0_2\ 90)_{16}$ CFRP SAMPLE

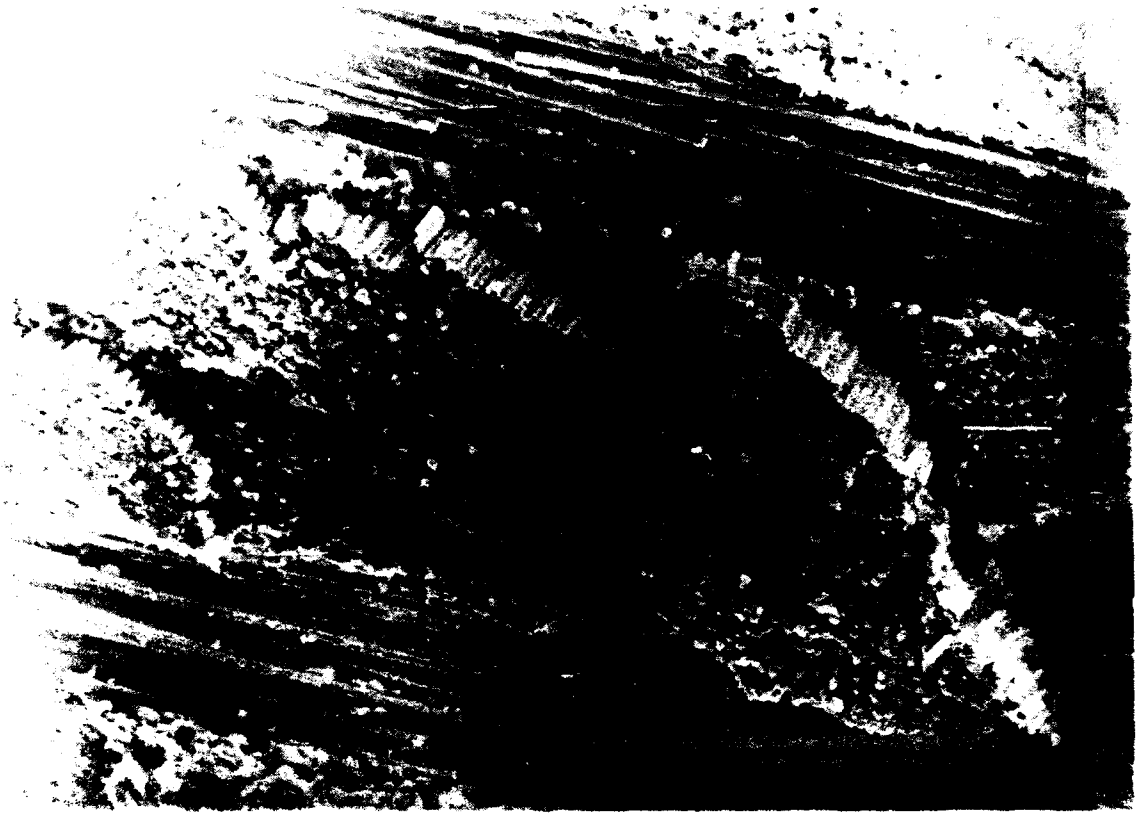

(x 150)

FIG. 28 FRACTURE SURFACE OF $(0_2/90)_{16}$ CFRP SAMPLE

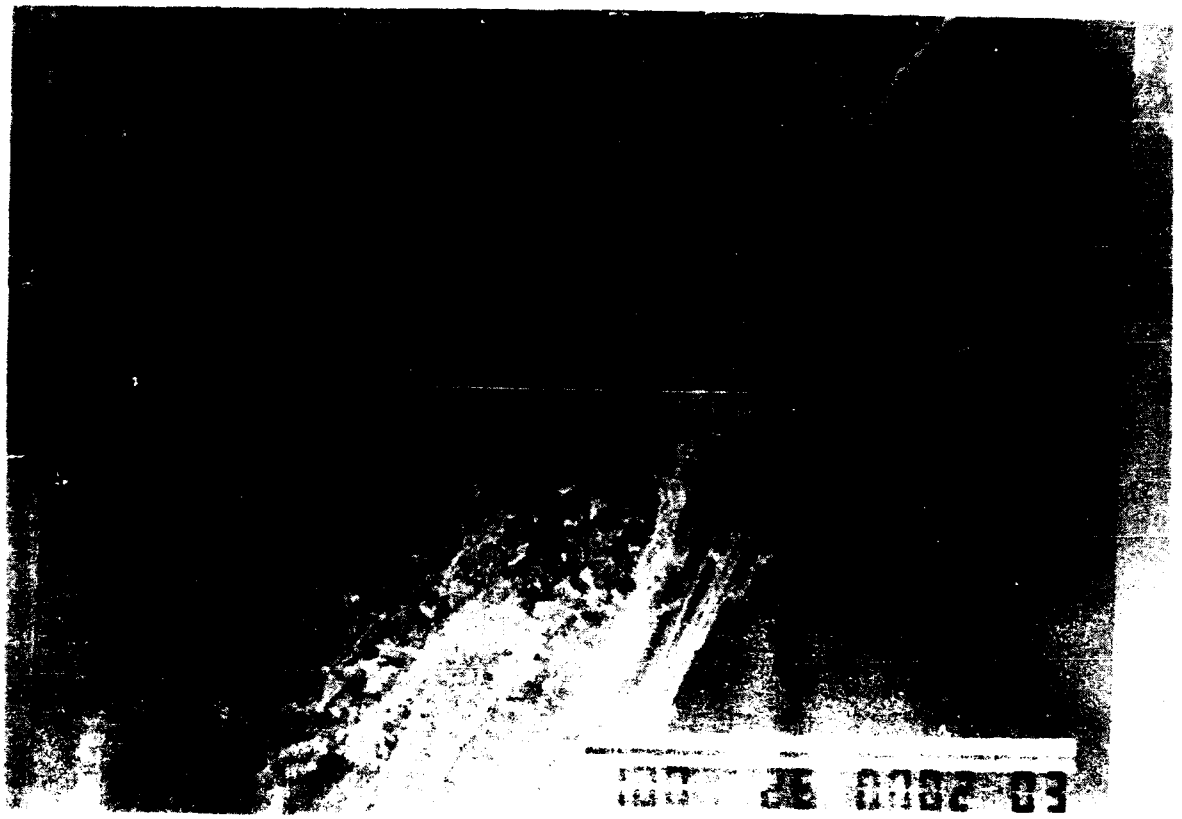

FIG. 29 KINK BANDS WITH $(0_2)_{16}$ C-FRP SAMPLE

FIG. 30

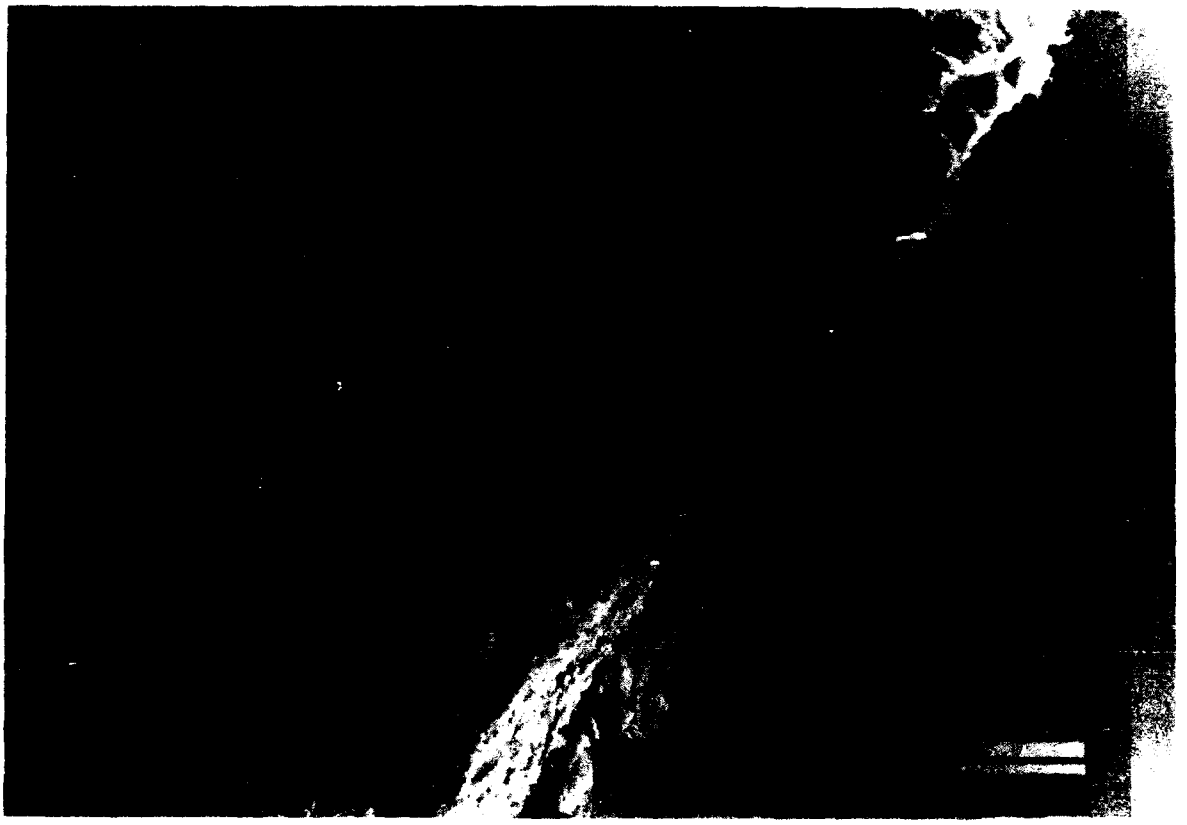

(x 200)

FIG. 30 KINK BANDS WITHIN $(0_2\ 90)_{16}$ CFRP SAMPLE

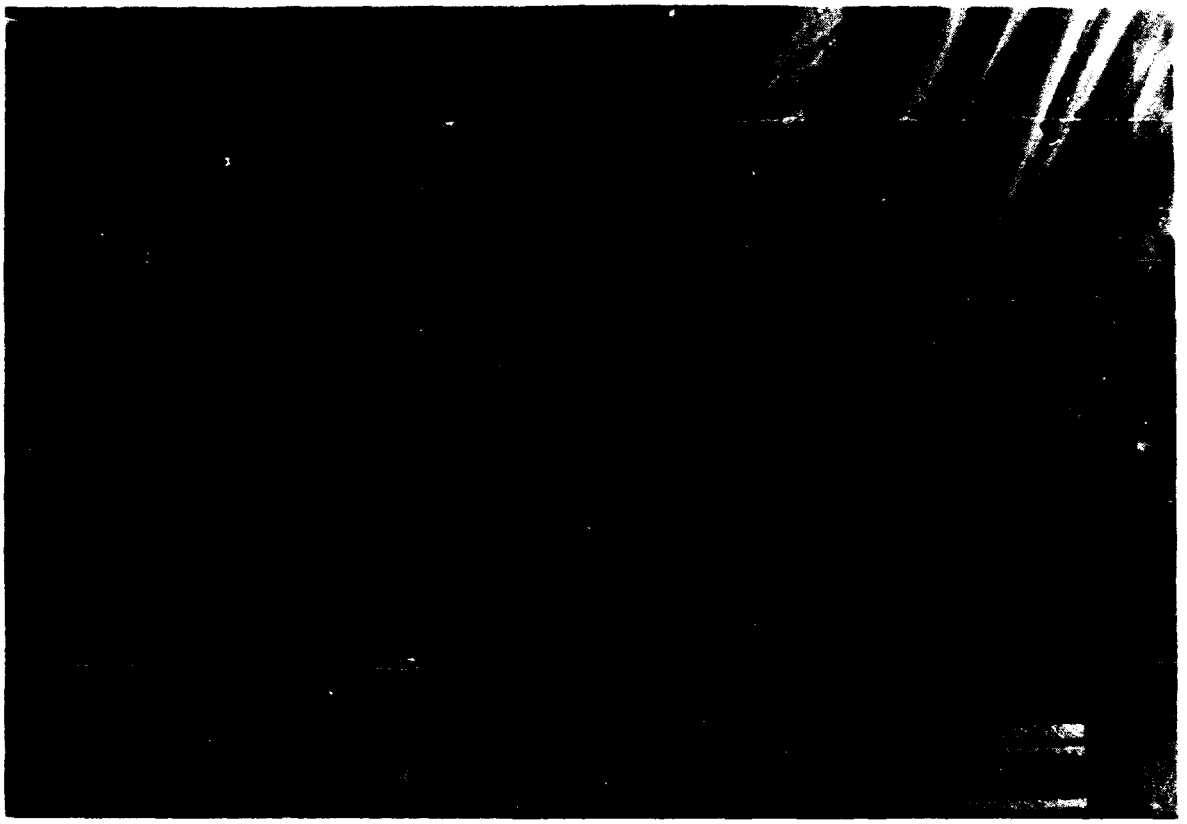

(x 350)

FIG. 31 KINK BANDS WITHIN $(0_2 90)_{16}$ CFRP SAMPLE

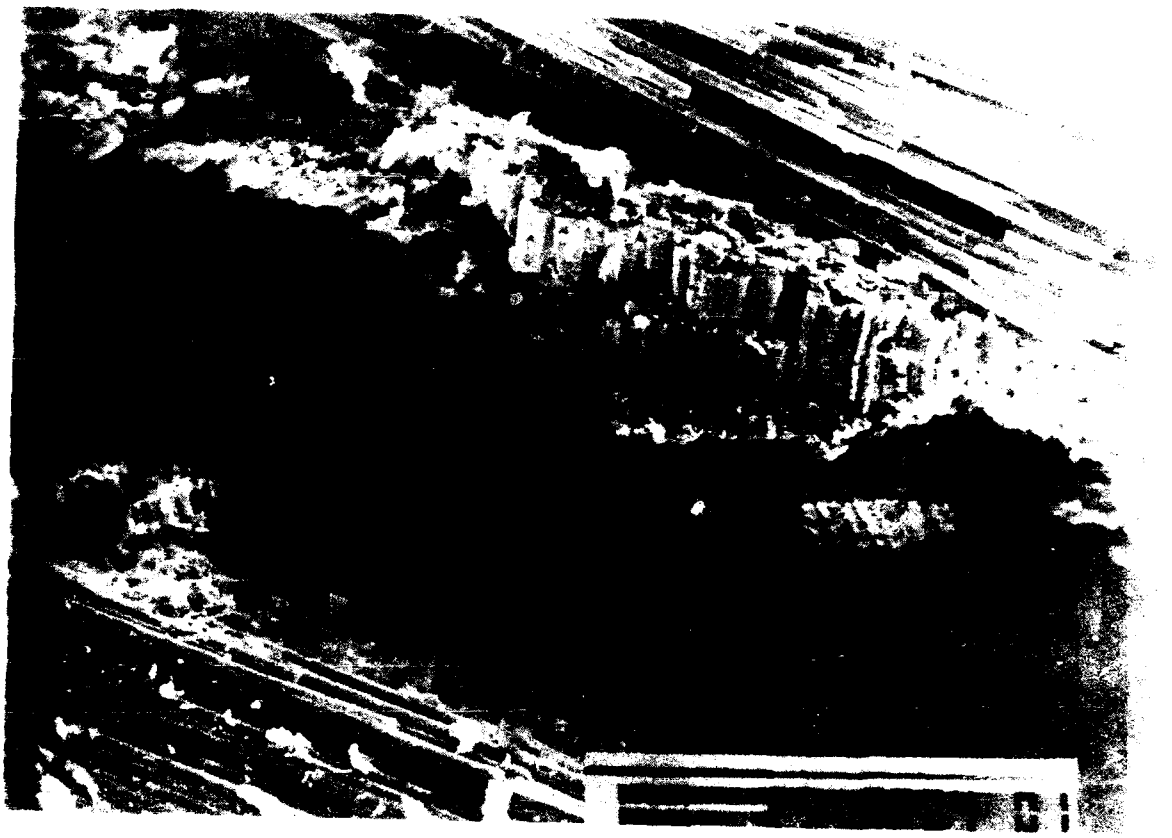

FIG 32 KINK BANDS WITHIN $(0_2 90_{16})_s$ CFRP LAMINATE

FIG. 33

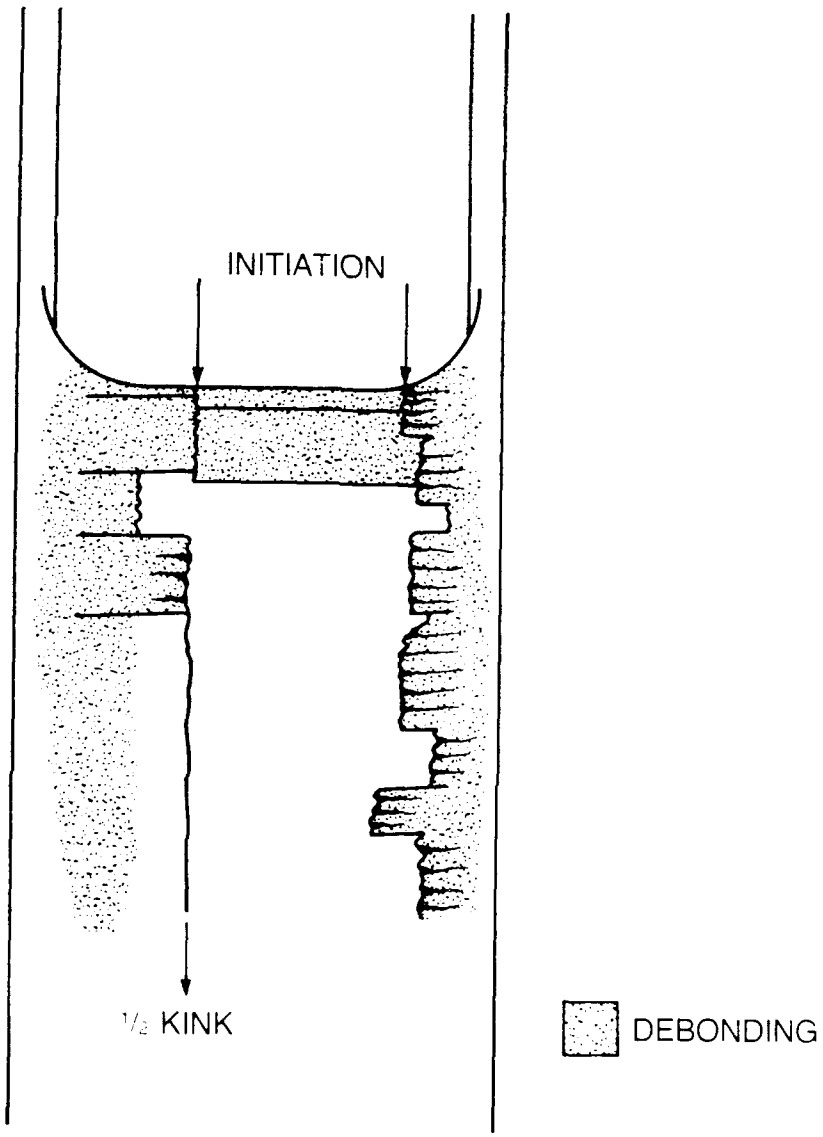

FIG. 33 NOTCH SURFACE OF $(0_2/90)_{16}$ GRP SPECIMEN

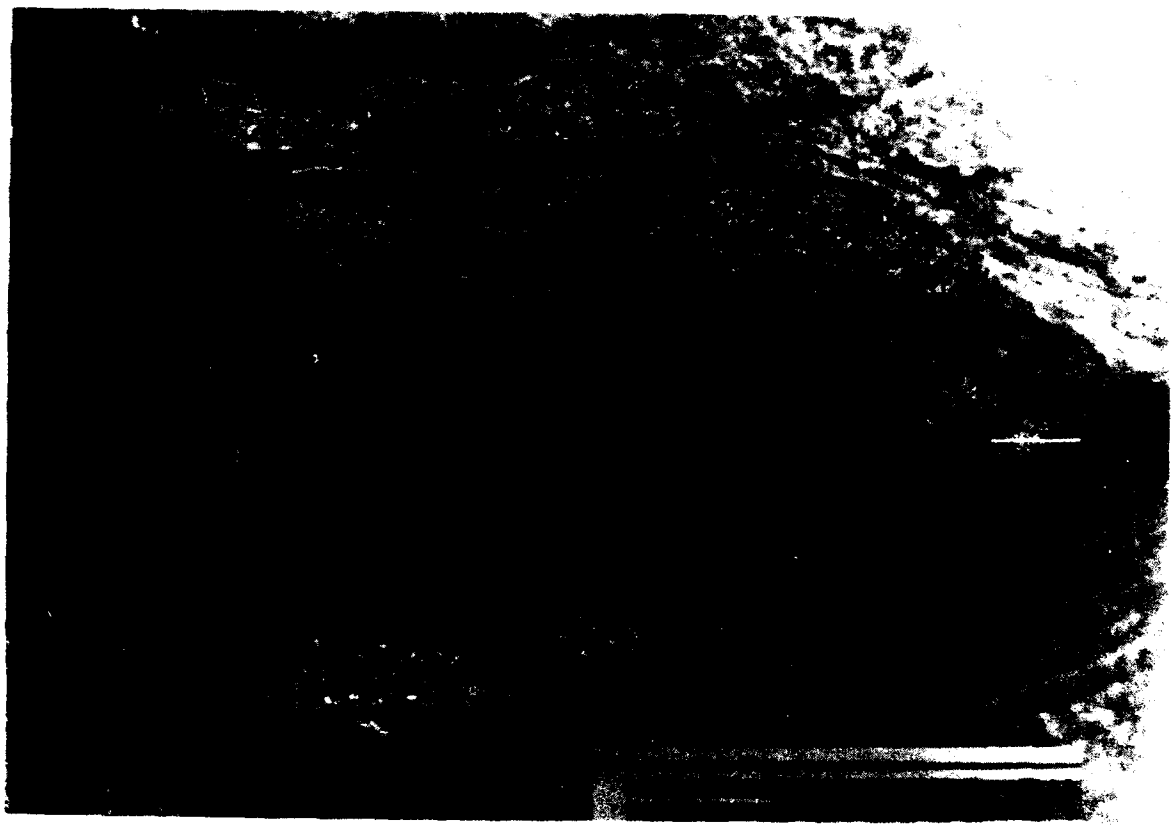

FIG. 34 FRACTURE SURFACE IN $(0_2/90)_{16}$ GRP SPECIMEN

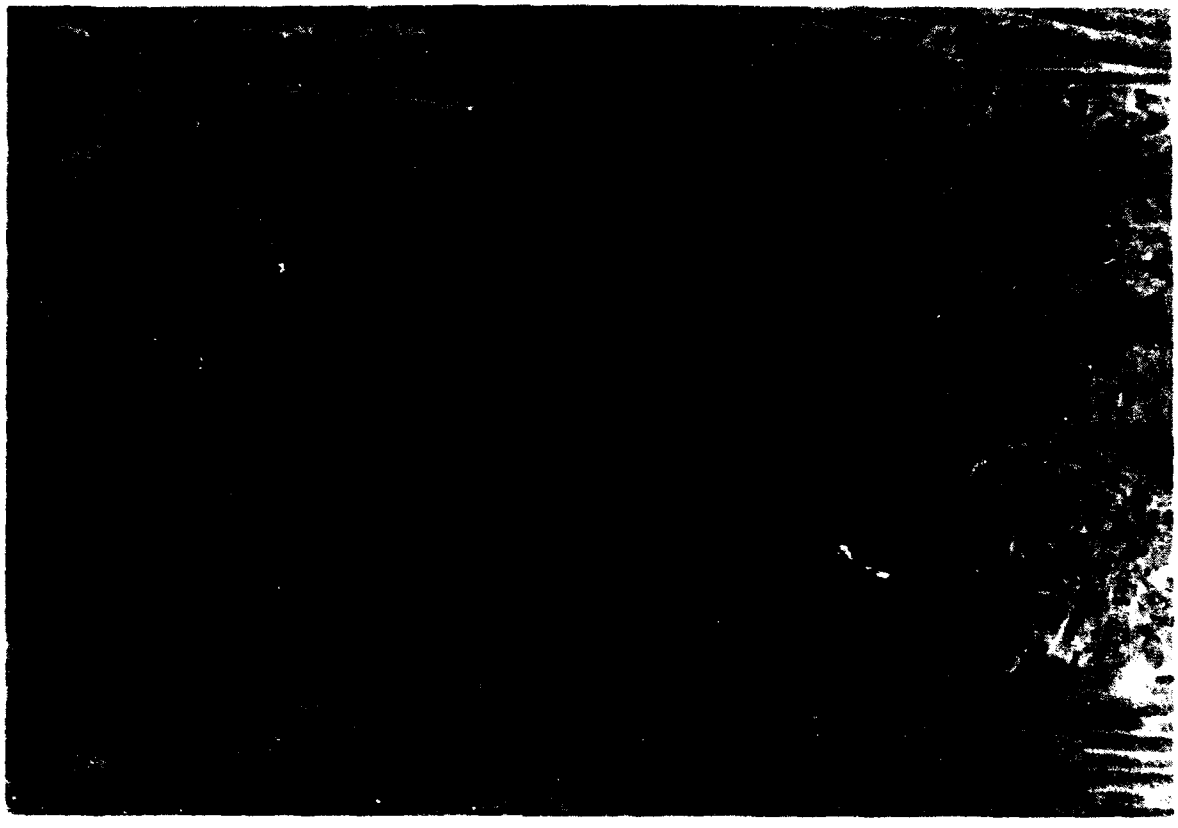

FIG. 35 FRACTURE SURFACE OF $[0_2/90]_{16}$ GRP SPECIMEN

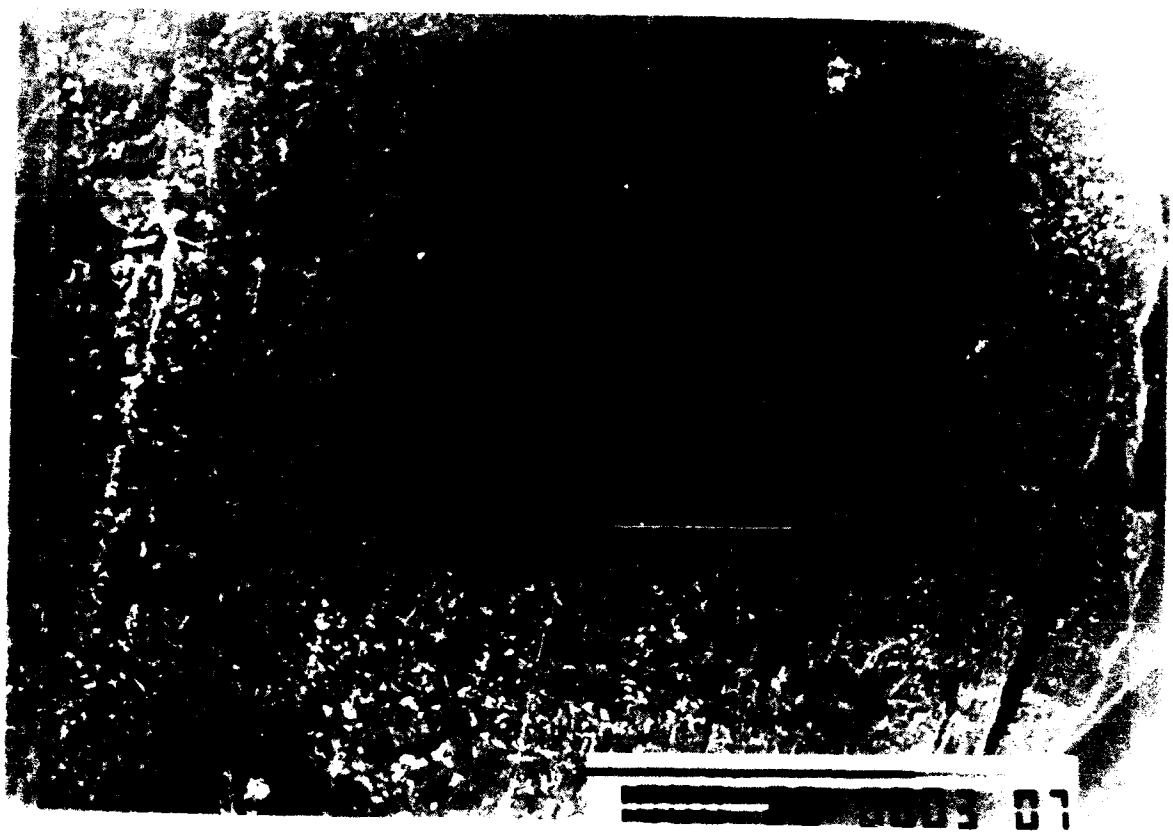

×35

FIG. 36 NOTCH SURFACE IN $(0_2 \pm 45)_{24}$ CFRP SPECIMEN SHOWING EXTENSIVE SPLITTING AT INTERFACES

FIG. 37

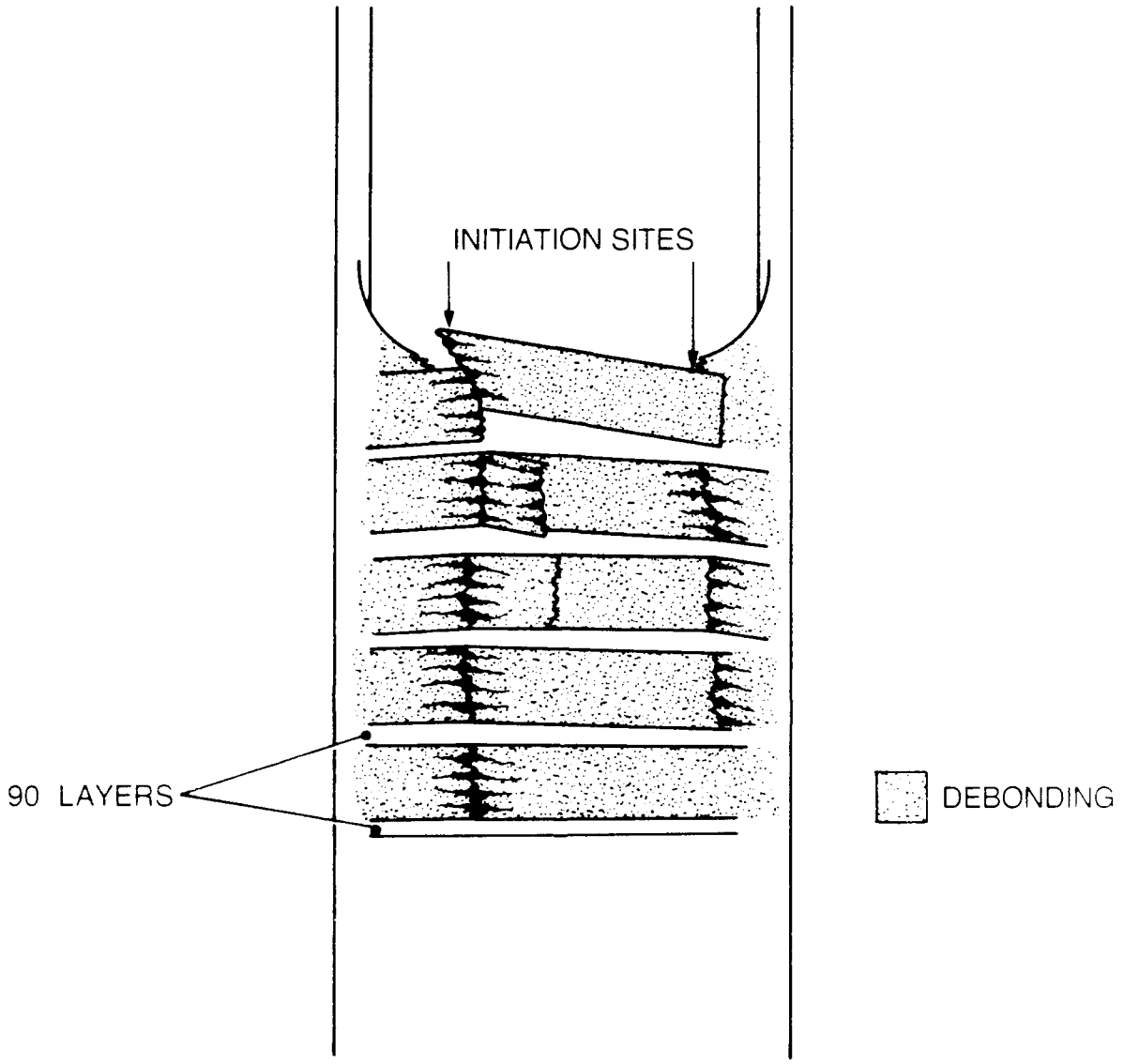

FIG. 37 NOTCH SURFACE OF $(0_4/90)_{24}$ GRP SPECIMEN

FIG. 38 FRACTURE SURFACE OF UNIDIRECTIONAL CFRP SPECIMEN SHOWING KINK BAND SIZES

FIG. 39 FRACTURED SURFACE OF UNIDIRECTIONAL CFRP SPECIMEN SHOWING KINK BAND SIZES

(x 500)

FIG. 40 FRACTURE SURFACE OF UNIDIRECTIONAL CFRP SPECIMEN, SHOWING MATRIX CRUSHING

ANNEX A

EULER BUCKLING

The equation of Euler, when applied to a composite reinforced with parallel fibres can be expressed as:

$$\sigma_f = \frac{\pi^2 E_f}{(l/k)^2} \text{ or } l = \pi k \sqrt{E_f/\sigma_f}$$

where σ_f is the fibre strength, E_f the fibre modulus, l the buckle wavelength (twice the kink band width), and k the radius of gyration of the fibre (in this case one quarter of the fibre diameter).

REPORT DOCUMENTATION PAGE

Overall security classification of the sheet: Unlimited

1. DRIC Reference Number (if known)
2. Originator's Reference Report 1/90
3. Report Security Classification Unlimited
4. Month April
5. Year 1990
6. Originator's Name, Location and Code Ministry of Defence, Royal Armament Research and Development Establishment, Waltham Abbey, Essex, 7699700E
7. Monitoring Agency Name, Location and Code
8. Title Work of Fracture of Composites in Axial Compression - Measurement and Origins
9. Title Classification Unlimited
10. Foreign Title
11. Conference Details
12. Contract Number and Period
13. Project
14. Other References
15. Author(s) N J Savage
16. Pagination and Ref 53pp 17 refs
17. Abstract Composite materials are being introduced into weapon systems and launch platforms of many kinds, increasingly as thick sections which accept high compressive stress. A common mode of failure is then by kink band propagation, arising from holes or other stress-raisers. The fibres broken in the process then cause weakness in tension as well. The tolerance of stress-raisers depends upon the energy required to propagate such kink bands. This report shows how to determine and to adjust this compressive work of fracture, and suggests how much energy different mechanisms may contribute. The work can be as little as 2-3J/sq.cm. when it is concentrated in a narrow band. Multiple kink bands may require up to 400J/cu.cm. for continuous crushing, an important ballistic feature if it can be sustained.
18. Abstract Classification Unlimited
19. Descriptors Composite materials, Fracture properties, Fractures - materials, Weapon systems, Stress analysis, Compressive properties, Failure, Measurement.
20. Release Authority